Business and Financial Cycles: an Unobserved Components Models Perspective

Gerhard Rünstler* Marente Vlekke

European Central Bank

October 2015

Abstract

We use multivariate unobserved components models to estimate trend and cyclical components in GDP, credit volumes and house prices for the U.S. and the five largest European economies. With the exception of Germany, we find large and long cycles in the financial series, which are highly correlated with a medium-term component in GDP cycles. Differences across countries in the length and size of cycles appear to be related to the properties of national housing markets. The precision of pseudo real-time estimates is roughly comparable to that of GDP cycles.

Keywords: Unobserved components models, business cycles, financial cycles

JEL classification: C35, E35, G02

*corresponding author: gerhard.ruenstler@ecb.europa.eu, European Central Bank, Sonnemannstrasse 20, D-60314 Frankfurt am Main. The views expressed in this paper are those of the authors and do not necessarily reflect the views of the ECB. The authors would like to thank Siem Jan Koopman, Bernd Schwaab, Yves Schüler, Peter Welz, and the participants of an internal ECB seminar for helpful discussions.

1 Introduction

The role of the financial sector in the creation and propagation of economic fluctuations is at the heart of both macroeconomic research and of considerations about the re-design of economic policy after the financial crisis. Given the key role of the leverage cycle in the emergence of financial imbalances (Geanakoplos, 2009; Jordà et al., 2014), an important element in these discussions is macro-prudential policies aimed at dampening cyclical fluctuations in credit volumes and residential property prices (Cerutti et al., 2015). Clearly, the implementation of such policies requires forming a view on the cyclical stance of these financial series.[1]

Against this background, recent studies have argued that post-war credit volumes and house prices in advanced economies contain pronounced medium-term cyclical components. These studies rely on univariate detrending methods, such as turning point analysis (Claessens et al., 2011, 2012), univariate band-pass filters (Aikman et al., 2015), or both (Drehmann et al., 2012; Schüler et al., 2015). Band-pass filters are usually applied with a frequency band of 32 to 120 quarters, but some studies use spectral methods to search for optimal frequency bands. A few studies apply univariate structural time series models (De Bonis and Silvestrini, 2013; Galati et al., 2015). One study using a multivariate approach is limited to U.S. data (Chen et al., 2013).

In this paper, we apply versions of multivariate structural time series models (STSMs), as introduced by Harvey and Koopman (1997), to estimate trend and cyclical components in real GDP, real credit volumes, and real residential property prices. We use quarterly data from 1973 Q1 to 2014 Q4 for the U.S. and the five largest economies in Europe. We are interested in two particular questions that are of relevance to macro-prudential policies: first, what is the relationship between financial and business cycles? And, second, how does the reliability of pseudo real-time estimates of financial cycles relate to that of business cycles? Understanding the relationship between financial and business cycles is important for the coordination of macro-prudential and monetary policies, while the need for reliable real-time estimates is apparent.

[1] See also Giese et al. (2014) for a discussion of the role of the credit-to-GDP gap in setting counter-cyclical capital buffers and Alessi and Detken (2014) for its use as an early warning indicator of financial crises.

We use the multivariate STSM because it provides a model-based approach to the estimation of the appropriate cyclical frequency bands and of cyclical co-movements. Non-parametric filters rely on pre-specified frequency bands, which implies a risk of missing parts of cyclical dynamics or, conversely, of obtaining spurious cycles (e.g. Harvey and Jäger, 1992). For instance, while Drehmann et al. (2012) regard financial and business cycles as *"different phenomena"*, such finding emerges from their choice of frequency bands for the extraction of GDP (8 to 32 quarters) and financial cycles (32 to 120 quarters): once the filter bands do not overlap, estimates of the two cycles are uncorrelated by construction. Schüler et al. (2015) address this deficiency by deriving the frequency bands from cross spectral densities, but this ignores information in the auto spectra. Similarly, turning point analysis is based on ad hoc assumptions and gives a limited characterisation of cyclical properties. Studies based on this method conclude that GDP recessions are particularly deep when accompanied by troughs in financial cycles (Claessens et al., 2012).

We extend the standard STSM in various ways to account for the different cyclical dynamics of GDP and the financial series and for the particularly high persistence in financial cycles. Further, we follow Rünstler (2004) in modelling phase shifts among cyclical components. Our study also builds on Chen et al. (2013) and Galati et al. (2015). Galati et al. (2015) estimate financial cycles in the major economies from univariate STSMs. Chen et al. (2013) apply a multivariate approach to U.S. data and report high coherences between GDP and financial cycles.

We use the model also to assess the properties of pseudo real-time estimates. Estimating medium-term cycles from 45 years of data may be regarded as a somewhat courageous undertaking, in particular when it comes to real-time estimates. We conduct a Monte Carlo study to learn about the precision of estimates of financial cycles in comparison with the traditional business cycles. We complement this with inspecting the subsequent revisions to the real-time estimates, that emerge once the information set is enlarged with further observations.

Our main findings are as follows. First, we find long and large cycles in the financial series, but also some important differences across countries. For the U.S., Italy and France, the estimated average cycle length is 12 to 15 years. Standard deviations of credit cycles range from 4% to 6%, those of house prices from 10% to 12%. Financial cycles are larger and longer for the U.K. and

Spain, while they are very small and short for Germany. Second, these differences correspond closely to the shares of private home ownership in national housing markets: financial cycles are larger and longer for countries with higher shares.

Third, financial cycles are closely related to a medium-term component in GDP cycles. Estimating the GDP cycles in a multivariate model jointly with the financial cycles emphasises medium-term frequencies and results in average cycle lengths outside the range of 8 to 32 quarters that is usually employed with band-pass filters for business cycles. We find the coherences between the three cycles to be high at frequencies lower than 32 quarters, but more moderate for the traditional business cycle frequencies. Further, house price cycles are contemporaneous to GDP cycles, while credit cycles tend to lag the latter.

Fourth, the uncertainty of real-time estimates of financial cycles is comparable to the one of traditional business cycles, when measured relative to the size of the cycles. Estimates of long cycles are subject to higher uncertainty. However, financial cycles are also larger, while trends remain comparatively smooth, which results in more favourable signal-to-noise ratios. In line with studies on the business cycle (e.g. Rünstler, 2002; Basistha and Startz, 2008; Trimbur 2009), we find that the multivariate STSM provides more precise real-time estimates than the univariate STSM and the band-pass filter.

The paper is organised as follows. Section 2 discusses the multivariate STSM used in our analysis. Section 3 presents estimates of GDP and financial cycles for the six countries under investigation. Section 4 discusses the precision of estimates. Section 5 concludes the paper.

2 Methodology

Section 2.1 reviews the multivariate structural time series model (STSM) introduced by Harvey and Koopman (1997). Section 2.2 discusses two extensions of the standard model, which account for the different dynamics of business and financial cycles and the high persistence of the latter. Section 2.3 turns to estimation and testing.

2.1 The Multivariate Structural Time Series Model

Consider a vector of n time series $\mathbf{x}_t' = (x_{1,t}, ..., x_{n,t})'$ with observations ranging from $t = 1, \ldots, T$. The multivariate STSM proposed by Harvey and Koopman (1997) is designed to decompose $\mathbf{x}_t$ into trend, $\boldsymbol{\mu}_t$, cyclical, $\mathbf{x}_t^C$, and irregular components, $\boldsymbol{\varepsilon}_t$,

$$\mathbf{x}_t = \boldsymbol{\mu}_t + \mathbf{x}_t^C + \boldsymbol{\varepsilon}_t \ . \tag{1}$$

The $n \times 1$ vector $\boldsymbol{\varepsilon}_t$ of irregular components is normally and independently distributed with mean zero and $n \times n$ covariance matrix Σ_ε, $\boldsymbol{\varepsilon}_t \sim \text{NID}(\mathbf{0}, \Sigma_\varepsilon)$. The $n \times 1$ vector $\boldsymbol{\mu}_t$ of stochastic trend components is defined as

$$\begin{aligned} \Delta\boldsymbol{\mu}_t &= \boldsymbol{\beta}_{t-1} + \boldsymbol{\eta}_t, & \boldsymbol{\eta}_t &\sim \text{NID}(\mathbf{0}, \Sigma_\eta) \ , \\ \Delta\boldsymbol{\beta}_t &= \boldsymbol{\zeta}_t, & \boldsymbol{\zeta}_t &\sim \text{NID}(\mathbf{0}, \Sigma_\zeta) \ , \end{aligned} \tag{2}$$

where level $\boldsymbol{\eta}_t' = (\eta_{1,t}, ..., \eta_{n,t})'$ and slope innovations $\boldsymbol{\zeta}_t' = (\zeta_{1,t}, ..., \zeta_{n,t})'$ are normally and independently distributed with $n \times n$ covariance matrices Σ_η and Σ_ζ, respectively.

Cyclical components $\mathbf{x}_t^C = (x_{1,t}^C, ..., x_{n,t}^C)'$ are modelled from stochastic cycles. The stochastic cycle (SC) is defined as a bivariate stationary stochastic process for $\widetilde{\boldsymbol{\psi}}_{i,t} = (\psi_{i,t}, \psi_{i,t}^*)'$,

$$\left(I_2 - \rho_i \begin{bmatrix} \cos\lambda_i & \sin\lambda_i \\ -\sin\lambda_i & \cos\lambda_i \end{bmatrix} L \right) \begin{bmatrix} \psi_{i,t} \\ \psi_{i,t}^* \end{bmatrix} = \begin{bmatrix} \kappa_{i,t} \\ \kappa_{i,t}^* \end{bmatrix} \ , \tag{3}$$

with decay $0 < \rho_i < 1$ and frequency $0 < \lambda_i < \pi$. I_2 denotes the 2×2 identity matrix, while L is the lag operator. Cyclical innovations $\widetilde{\boldsymbol{\kappa}}_{i,t} = (\kappa_{i,t}, \kappa_{i,t}^*)'$ are distributed as $\widetilde{\boldsymbol{\kappa}}_{i,t} \sim \text{NID}(\mathbf{0}, \sigma_{\kappa,ii}^2 I_2)$.

The autocovariance generating function (ACF) $\widetilde{V}_{ii}(s) = \mathbb{E}\left[\widetilde{\boldsymbol{\psi}}_{i,t}\widetilde{\boldsymbol{\psi}}_{i,t-s}'\right]$ for $s = 0, 1, 2, \ldots$, is given by dampened cosine and sine waves of period $2\pi/\lambda_i$,

$$\widetilde{V}_{ii}(s) = \sigma_{\kappa,ii}^2 h(s; \rho_i) T^+(s\lambda_i) \ , \text{ where} \tag{4}$$

$$T^+(s\lambda_i) = \begin{bmatrix} \cos(s\lambda_i) & \sin(s\lambda_i) \\ -\sin(s\lambda_i) & \cos(s\lambda_i) \end{bmatrix} \ ,$$

with scalar function $h(s; \rho_i) = (1 - \rho_i^2)^{-1} \rho_i^s$ and orthonormal, skew-symmetric matrix $T^+(s\lambda_i)$.

The spectral generating function (SGF) $\widetilde{G}_{ii}(\omega)$ of $\widetilde{\psi}_{i,t}$ is discussed in Annex A. It is hump-shaped with a peak close to λ_i, while the dispersion around the peak is determined by ρ_i. The stochastic cycle is therefore well-suited for extracting a certain frequency band of the spectrum.[2] If ρ converges to 1, together with $\sigma^2_{\kappa,ii}$ converging to 0, the SC becomes deterministic and the spectrum collapses to a single point, $\widetilde{G}_{ii}(\omega) = 0$ for $\omega \neq \lambda$.

For the multivariate case, assume that the $n \times 1$ vector $\mathbf{x}_t^C$ of cyclical components is driven by n independent stochastic cycles. Define the $2n \times 1$ vector $\widetilde{\boldsymbol{\psi}}_t = (\boldsymbol{\psi}_t', \boldsymbol{\psi}_t^{*\prime})'$ with $\boldsymbol{\psi}_t = (\psi_{1,t}, ..., \psi_{n,t})'$ and $\boldsymbol{\psi}_t^* = (\psi_{1,t}^*, ..., \psi_{n,t}^*)'$. Equivalently, define the $2n \times 1$ vector of innovations $\widetilde{\boldsymbol{\kappa}}_t$ with covariance matrix $\mathbb{E}\left[\widetilde{\boldsymbol{\kappa}}_t \widetilde{\boldsymbol{\kappa}}_t'\right] = I_{2n}$. We specify cyclical components $\mathbf{x}_t^C$ as linear combinations of $\boldsymbol{\psi}_t$ and $\boldsymbol{\psi}_t^*$,

$$\mathbf{x}_t^C = (A, A^*)\widetilde{\boldsymbol{\psi}}_t \ , \tag{5}$$

where $A = (a_{ij})$ and $A^* = (a_{ij}^*)$ are general $n \times n$ matrices.

In empirical applications to the business cycle, this specification has so far been used under the assumption of so-called similar cycles, which amounts to the restriction of identical decays and frequencies $\rho_i = \rho$ and $\lambda_i = \lambda$ for $i = 1, \ldots, n$. This allows for expressing the dynamics of $\widetilde{\boldsymbol{\psi}}_t$ as

$$\left(I_{2n} - \rho \left[T^+(\lambda) \otimes I_n\right] L\right) \widetilde{\boldsymbol{\psi}}_{t-1} = \widetilde{\boldsymbol{\kappa}}_t \ . \tag{6}$$

As shown by Rünstler (2004), equation (5) introduces phase shifts between cyclical components. Specifically, the elements $V_{ij}^C(s)$ of the ACF $V^C(s)$ of $\mathbf{x}_t^C$ can be expressed as

$$V_{ij}^C(s) = h(s;\rho) r_{ij} \cos(\lambda(s - \theta_{ij})) \ , \tag{7}$$

where $r_{ij} = \sqrt{a_{ij}^2 + a_{ij}^{*2}}$ and $\theta_{ij} = \lambda^{-1} \arctan(a_{ij}^*/a_{ij})$ are derived from the elements of A and A^*. As discussed in Annex A, this property arises from the skew-symmetry of $T^+(s\lambda_i)$. Equation (5) implies that cyclical components are linear combinations of the elements of $\boldsymbol{\psi}_t$ and $\boldsymbol{\psi}_t^*$. Hence, from equation (4), with a non-zero A^*, cross-correlations among the elements of $\mathbf{x}_t^C$ emerge as mixtures of sine and cosine waves, which can be written as cosine waves subject to phase shifts.

[2] Harvey and Trimbur (2004) show that extensions of the above model involving higher-order trends and higher-order stochastic cycles converge towards optimal band-pass filters.

The skew-symmetry of $T_1^+(s\lambda_i)$ implies that $r_{ij} = r_{ji}$ and $\theta_{ij} = -\theta_{ji}$. It can also be shown that coherence and phase spectra at λ converge towards $\gamma_{ij} = r_{ij}/\sqrt{r_{ii}r_{jj}}$ and θ_{ij}, respectively, for $\rho \to 1$. Hence, r_{ij} and θ_{ij} have an interpretation as phase-adjusted covariances and phase shifts.

Identifiability requires certain restrictions to be imposed on (A, A^*). An identified representation is given by lower triangular matrices, $a_{ij} = 0$ for $i < j$ and $a^*_{ij} = 0$ for $i \leq j$ (see Rünstler, 2004).[3]

2.2 Extensions

We consider two extensions of the model of section 2.1, which are motivated by the findings of earlier studies and our own preliminary estimates.

First, given the emphasis of earlier studies on the different dynamics of business and financial cycles, we abandon the similar cycles assumption $\rho_i = \rho$ and $\lambda_i = \lambda$ for $i = 1, \ldots, k$. Hence, from equation (5), cyclical components $\mathbf{x}_t^C$ may load, via matrices A and A^*, on three latent independent stochastic cycles with potentially different dynamics. This allows for a flexible approach to modelling coherence and phase shifts between the elements of $\mathbf{x}_t^C$ at both business and financial cycle frequencies. However, while we abandon the assumption of overall similar cycles, we will test for pairwise similar dynamics and impose it on our final estimates if it is not rejected.

Second, to account for the high persistence of financial cycles, we expand the dynamics of the SC by adding a further (scalar) autoregressive root $0 < \phi_i < 1$, which gives rise to the specification

$$(1 - \phi_i L)\left(I_2 - \rho_i \begin{bmatrix} \cos\lambda_i & \sin\lambda_i \\ -\sin\lambda_i & \cos\lambda_i \end{bmatrix} L\right) \begin{bmatrix} \psi_{i,t} \\ \psi^*_{i,t} \end{bmatrix} = \begin{bmatrix} \kappa_{i,t} \\ \kappa^*_{i,t} \end{bmatrix} . \tag{8}$$

We refer to this process as the stochastic cycle with extended dynamics (SCE). As the SCE amounts to a scalar distributed lag of the SC in equation (3), it maintains many of its properties. Specifically, as long as ϕ_i is not too close to one, auto spectra remain hump-shaped. However, they are more dispersed around their peak and skewed towards somewhat higher mass at low frequencies. Morever, the above symmetry properties of the ACF are maintained: autocorrelations of $\psi_{i,t}$ and $\psi^*_{i,t}$ are identical, while their cross-correlations are skew-symmetric (see Annex A).

[3] see also Valle e Azevedo et al. (2006), Koopman and Valle e Azevedo (2008), and Moës (2012) for applications.

Our model consists of equations (1), (2), and (5). The elements $\widetilde{\boldsymbol{\psi}}_{i,t} = \left(\psi_{i,t}, \psi^*_{i,t}\right)$ of the $2n \times 1$ vector $\widetilde{\boldsymbol{\psi}}_t = (\boldsymbol{\psi}_t', \boldsymbol{\psi}_t^{*\prime})'$ follow stochastic processes as defined in equation (8) with covariance matrix $\mathbb{E}\left[\widetilde{\boldsymbol{\kappa}}_t \widetilde{\boldsymbol{\kappa}}_t{}'\right] = I_{2n}$. The model parameters are given by the elements of matrices Σ_η, Σ_ζ, and (A, A^*), together with ϕ_i, ρ_i, and λ_i, $i = 1, \ldots, n$. Two SCEs $\widetilde{\boldsymbol{\psi}}_{i,t}$ and $\widetilde{\boldsymbol{\psi}}_{j,t}$ are said to share similar dynamics if $\phi_i = \phi_j$, $\rho_i = \rho_j$, and $\lambda_i = \lambda_j$. The model is completed by the assumption that $\boldsymbol{\varepsilon}_t$, $\boldsymbol{\eta}_t$, $\boldsymbol{\zeta}_t$ and $\widetilde{\boldsymbol{\kappa}}_t$ are mutually uncorrelated.

Again, certain identifying restrictions on the elements of (A, A^*) in equation (5) are required. With non-similar cycles, it is sufficient to impose a normalisation of phase shifts, which can be achieved from $a^*_{ii} = 0$ for $i = 1, \ldots, n$. Additional restrictions are required in case a subset of SCEs share pairwise similar dynamics. As discussed in Annex A, they can be implemented by imposing lower triangularity on the corresponding sub-matrices of (A, A^*). If, for instance, SCEs 2 and 3 share similar dynamics, then identifiability is achieved from $a_{13} = a^*_{13} = 0$.

With non-similar cycles, the ACF $V^C(s)$ of cyclical components $\mathbf{x}^C_t$ emerges as a mixture of cosine waves of different lengths, and convenient closed-form analytical expressions for cross-correlations do no longer exist. To characterise cyclical co-movements we therefore calculate the multivariate spectral generating function $G^C(\omega)$ of $\mathbf{x}^C_t$ from our parameter estimates and report various statistics obtained from the latter.[4] The derivation of $G^C(\omega)$ is discussed in Annex A.

Denote the elements of $G^C(\omega)$ with $G^C_{ij}(\omega)$, $i, j = 1, \ldots, n$. We obtain the average frequencies λ^G_i of cyclical components $x^C_{i,t}$ and the average coherences and phase shifts among them from the weighted integrals

$$\left(\int_0^\pi \sqrt{G^C_{ii}(\omega) G^C_{jj}(\omega)}\, \mathrm{d}\,\omega \right)^{-1} \int_0^\pi \varphi_{ij}(\omega) \sqrt{G^C_{ii}(\omega) G^C_{jj}(\omega)}\, \mathrm{d}\,\omega, \tag{9}$$

based on auto spectra $G^C_{ii}(\omega)$. To calculate λ^G_i we set $\varphi_{ii}(\omega) = \omega$. For brevity, we will refer to $2\pi/4\lambda^G_i$ as the (annual) average cycle length of series i. To calculate average coherence and phase shifts functions $\varphi_{ij}(\omega)$ represent either coherence or phase spectra, which are derived from the respective elements of $G^C(\omega)$.

[4] This approach has been used, among others, by King and Watson (1996) in a VAR context.

2.3 Estimation and Testing

We estimate the model via maximum likelihood by casting the equations in state-space form

$$\mathbf{x}_t = Z\alpha_t + \boldsymbol{\varepsilon}_t,$$
$$\alpha_{t+1} = W\alpha_t + \xi_t$$

and by applying the prediction error decomposition of the Kalman filter. The associated smoothing algorithms (see e.g. Durbin and Koopman, 2001) then provide minimum mean square linear estimates $\alpha_{t|s} = \mathbb{E}[\alpha_t|\mathcal{X}_s]$ of the state vector and their covariance $P_{t|s}$ for arbitrary information sets $\mathcal{X}_s = \{\mathbf{x}_\tau\}_{\tau=1}^{s}$with $s > t$. Studies usually report the most efficient full-sample estimates $\alpha_{t|T}$. In order to assess the properties of real-time estimates we will also inspect real-time estimates $\alpha_{t|t}$ and the subsequent evolution of smoothed estimates $\alpha_{t|t+h}$ for fixed $h > 0$.

We obtain preliminary estimates of key parameters and carry out tests on cyclical dynamics from the application of univariate STSMs to each series. LR tests on similar dynamics under the full model are not feasible. We therefore conduct likelihood ratio (LR) tests on overall and pairwise similar dynamics from joint estimation of the univariate STSMs under the respective restrictions. We impose pairwise similar dynamics if the restrictions are not rejected.[5]

3 Stylised Financial Cycles Facts

We apply the multivariate STSM as described in section 2 to real GDP (Y_t), real total credit volumes (C_t), and an index of real residential property prices (P_t). We use quarterly data for the U.S., the U.K., Germany, France, Italy, and Spain. The data range from 1973 Q1 to 2014 Q4.[6] We take real GDP and GDP deflator series from the OECD main economic indicators database and nominal total credit volumes and nominal residential property prices from BIS databases.

[5] As discussed in section 2.2, similar cycles require some additional identifying restrictions to be imposed on the elements of A and A^*. The test statistic therefore has a non-standard test distribution under the null hypothesis.

[6] Our data start in 1970 Q1 for most countries, but house price data are of poor quality in the initial years of the sample. We therefore start estimation in 1973 Q1. We choose total credit instead of total bank credit because the latter series do not capture mortgages funded via securitisation (ECB, 2008). Quarterly data for mortgage credit, in turn, start only in 1980 or even 1999.

We deflate the latter two series with the GDP deflator.

We start with fitting the univariate STSM, as given by equations (1), (2), and (8). We conduct likelihood ratio (LR) tests on cyclical dynamics from joint estimation of the univariate models for the three series. The joint null hypothesis of $\phi_i = 0$ for $i = \{1, 2, 3\}$ is rejected for all countries at extremely high significance levels, while estimating the model under the null leaves high autocorrelation in prediction errors. Subsequent LR tests of the similar cycles restriction either reject or are close to rejecting the restriction of similar cycles between all three series at the 10% level. Conversely, pairwise similar dynamics between credit volumes and house prices is accepted at convenient significance levels.

We therefore estimate the multivariate STSM under the restriction that SCEs 2 and 3 share similar cyclical dynamics, $\phi_2 = \phi_3$, $\rho_2 = \rho_3$, and $\lambda_2 = \lambda_3$. Moreover, we restrict the standard deviation of slope innovations to credit volumes and house prices to a value of $\sigma_\zeta = 0.001$, close to the upper range of unrestricted estimates of these parameters across countries. For Spain, we impose values of $\rho_2 = 0.98$ and $\sigma_\zeta = 0.0025$. With these restrictions, which assume slopes to be somewhat more volatile than the unrestricted estimates, we aim at improving the comparability of results across countries and at insuring against potentially spurious estimates of overly long and large estimates of financial cycles. The results for unrestricted estimates are very similar. Estimates of the irregular component $\boldsymbol{\varepsilon}_t$ turn out to be very small, and we restrict them to zero.[7]

The left-hand panels of Table 1 and 2 show the parameter estimates of the univariate STSMs under the similar cycles restriction on credit volumes and house prices, and with restricted standard deviations of slope innovations. The estimates reveal pronounced cycles in the financial series with average annual cycle lengths $2\pi/4\lambda^G$, as calculated from the SGF, of in between 15.6 and 16.5 years for all countries but Germany (Table 2). For the latter, the estimated average annual cycle length is 8.2 years and the standard deviations of cycles are comparatively small. Estimates for GDP cycles differ more widely across countries. They are in a range of 5.1 to 5.9 years for Germany and Italy, 7.7 to 9.5 years for the U.S., U.K., and France, and 12.3 years for Spain.

[7]Supplement A to this paper shows more detailed results for both restricted and unrestricted estimates together with graphs of trend and cyclical components and prediction errors.

Table 1: Main Parameter Estimates from Univariate and Multivariate STSMs

	Univariate STSM						Multivariate STSM					
	Stochastic Cycles				Trend innovations		Stochastic Cycles				Trend innovations	
	ϕ	ρ	$2\pi/4\lambda$		σ_η	σ_ζ	ϕ	ρ	$2\pi/4\lambda$		σ_η	σ_ζ
United States												
$\psi_{1,t}$	0.483	0.935	8.995	Y_t	0.533	0.037	$\psi_{1,t}$	0.000	0.860	4.770	Y_t	0.000	0.031
$\psi_{23,t}$	0.920	0.945	12.514	C_t	0.244	0.100	$\psi_{23,t}$	0.859	0.956	10.795	C_t	0.000	0.100
				P_t	0.001	0.100					P_t	0.000	0.100
United Kingdom												
$\psi_{1,t}$	0.286	0.953	12.729	Y_t	0.000	0.049	$\psi_{1,t}$	0.000	0.931	8.192	Y_t	0.000	0.035
$\psi_{23,t}$	0.720	0.982	18.119	C_t	1.627	0.100	$\psi_{23,t}$	0.693	0.979	18.535	C_t	1.556	0.100
				P_t	1.269	0.100					P_t	1.138	0.100
Germany												
$\psi_{1,t}$	0.000	0.944	5.822	Y_t	0.730	0.021	$\psi_{1,t}$	0.000	0.630	5.427	Y_t	0.000	0.036
$\psi_{23,t}$	0.147	0.941	11.642	C_t	0.517	0.100	$\psi_{23,t}$	0.262	0.936	9.317	C_t	0.000	0.100
				P_t	0.002	0.100					P_t	0.000	0.100
France												
$\psi_{1,t}$	0.850	0.822	5.895	Y_t	0.292	0.031	$\psi_{1,t}$	0.000	0.892	3.187	Y_t	0.079	0.054
$\psi_{23,t}$	0.850	0.951	16.672	C_t	0.502	0.100	$\psi_{23,t}$	0.821	0.969	15.407	C_t	0.470	0.100
				P_t	0.304	0.100					P_t	0.289	0.100
Italy												
$\psi_{1,t}$	0.886	0.848	3.124	Y_t	0.449	0.050	$\psi_{1,t}$	0.000	0.912	2.972	Y_t	0.052	0.057
$\psi_{23,t}$	0.726	0.967	19.255	C_t	0.906	0.100	$\psi_{23,t}$	0.726	0.955	15.578	C_t	0.876	0.100
				P_t	0.000	0.100					P_t	0.208	0.100
Spain												
$\psi_{1,t}$	0.150	0.980	14.767	Y_t	0.000	0.050	$\psi_{1,t}$	0.000	0.936	3.331	Y_t	0.427	0.052
$\psi_{23,t}$	0.697	0.980	16.998	C_t	0.000	0.250	$\psi_{23,t}$	0.842	0.980	18.917	C_t	0.109	0.250
				P_t	0.861	0.100					P_t	0.450	0.100

The left-hand panel shows the parameter estimates from the univariate STSM under the restriction of similar cycles between credit volumes and house prices ($\psi_{2,t}$ and $\psi_{3,t}$). For the univariate STSM the stochastic cycles correspond to cyclical components in the series. The right-hand panel shows the estimates for the multivariate STSM. Parameters σ_η, and σ_ζ denote the standard deviations of trend and slope innovations, respectively, multiplied by 100. The estimates impose restrictions on σ_ζ for credit volumes and house prices.

In the multivariate STSM, the cyclical components x_{it}^C in the three series emerge as a mixture of the three stochastic cycles $\widetilde{\psi}_{i,t}$, $i = \{1, 2, 3\}$, as in equation (5). Hence, the parameter estimates

for the latent SCEs do not directly reflect the characteristics of cyclical components $\mathbf{x}_t^C$ and the interpretation of parameters differs from the univariate case. The parameter estimates are shown in the right-hand panel of Table 1. With the exception of Germany, SCEs $\widetilde{\boldsymbol{\psi}}_{2,t}$ and $\widetilde{\boldsymbol{\psi}}_{3,t}$ turn out to be long and persistent. Estimates of $2\pi/4\lambda$ are in between 10.7 and 18.9 years, while ρ_2 is estimated at around 0.95, and ϕ_2 attains values of 0.69 to 0.86. The first stochastic cycle, $\widetilde{\boldsymbol{\psi}}_{1,t}$, is considerably shorter and less persistent with estimates of $2\pi/4\lambda$ from 2.9 to 8.2 years. Parameter ϕ_1 turns out to be insignificant in all cases and we set it to zero.

The resulting properties of cyclical components x_{it}^C in the three series, as derived from the SGF are depicted in the right-hand panel of Table 2. Figure 1 plots the full-sample estimates $\widehat{\mathbf{x}}_{t|T}^C$ of the cyclical components.

Our main findings are as follows. First, financial cycles are generally larger and longer than GDP cycles, but there are substantial differences across countries. One may sort the countries into three groups, according to the lengths and standard deviations of financial cycles. Germany stands out with very short and small cyclical components in the financial series. The average cycle lengths of GDP and financial cycles are very similar, ranging from 6.2 to 7.1 years (parameter $2\pi/4\lambda^G$ in Table 2). Standard deviations of credit and house price cycles are estimated at 1.4% and 2.7%, respectively, in the same range as the standard deviation of the GDP cycle (2.1%).[8]

The U.S., France, and Italy form the centre group with financial cycles of considerable size and length. The average length of financial cycles ranges from 11.8 to 15.3 years; for GDP cycles, the estimates range from 8.7 for the U.S. to 12.5 years for France. Standard deviations of credit cycles range from 3.9% to 6.2%, those of house price cycles from 10.5% to 12.4%. This compares to standard deviations of GDP cycles of 2.5% to 2.9%.

The third group consists of the U.K. and Spain, for which financial cycles are particularly long and large. Estimates of the average cycle length range from 15.8 to 18.7 years. The standard deviations of house price cycles are estimated at 18.6% to 21.2%, those of credit cycles at 7.6%

[8]For Germany, the BIS house price series differs substantially from the one published by the OECD. The latter refers to house prices in urban areas only (Scatigna et al., 2014). The OECD series gives rise to a somewhat longer and larger cycle, but it still remains very small compared to the other countries.

and 14.0%, respectively. In addition, the GDP cycles are longer and larger: the average cycle lengths are at 13.5 and 17.6 years, respectively, while standard deviations attain a value of 4.1%.

Table 2: Properties of Cyclical Components

	Univariate STSM			Multivariate STSM						
	$2\pi/4\lambda^G$	σ^C		$2\pi/4\lambda^G$	σ^C			Phase		
United States							Y_t^C	C_t^C	P_t^C
Y_t	7.718	2.119	Y_t	8.735	2.535		Y_t^C		1.432	0.575
C_t	16.551	5.616	C_t	11.792	3.913	Coh	C_t^C	0.805		-1.409
P_t	16.551	16.734	P_t	12.105	12.053		P_t^C	0.726	0.509	
United Kingdom							Y_t^C	C_t^C	P_t^C
Y_t	9.527	2.976	Y_t	13.478	4.094		Y_t^C		1.976	0.739
C_t	16.554	9.220	C_t	15.837	7.683	Coh	C_t^C	0.532		-1.274
P_t	16.554	21.514	P_t	16.476	18.593		P_t^C	0.927	0.598	
Germany							Y_t^C	C_t^C	P_t^C
Y_t	5.135	1.360	Y_t	6.336	2.147		Y_t^C		1.076	1.132
C_t	8.172	1.215	C_t	6.193	1.431	Coh	C_t^C	0.740		0.158
P_t	8.172	2.774	P_t	7.112	2.712		P_t^C	0.610	0.683	
France							Y_t^C	C_t^C	P_t^C
Y_t	8.584	1.692	Y_t	12.572	2.678		Y_t^C		2.669	-0.705
C_t	16.509	4.917	C_t	15.057	5.099	Coh	C_t^C	0.875		-4.455
P_t	16.509	9.900	P_t	15.250	10.551		P_t^C	0.734	0.572	
Italy							Y_t^C	C_t^C	P_t^C
Y_t	5.931	1.917	Y_t	9.240	2.918		Y_t^C		1.492	5.407
C_t	16.539	7.517	C_t	13.354	6.220	Coh	C_t^C	0.569		2.441
P_t	16.539	15.588	P_t	13.553	12.370		P_t^C	0.727	0.426	
Spain							Y_t^C	C_t^C	P_t^C
Y_t	12.266	3.021	Y_t	17.582	4.118		Y_t^C		2.959	-0.837
C_t	15.627	8.050	C_t	18.690	14.038	Coh	C_t^C	0.808		-7.116
P_t	15.627	23.173	P_t	17.075	21.191		P_t^C	0.740	0.437	

The left-hand panel shows estimates of the average annual length $2\pi/4\lambda^G$ and the standard deviation σ^C (multiplied by 100) of cyclical components from the univariate STSM. The right-hand panel shows the corresponding estimates from the multivariate STSM and matrices with average coherences in the lower left and average phase shifts (in annual terms) in the upper right. A positive value of the phase shift means that series row leads series column. All statistics are derived from the SGF described in section 2.2.

Figure 1: Smoothed Cyclical Components

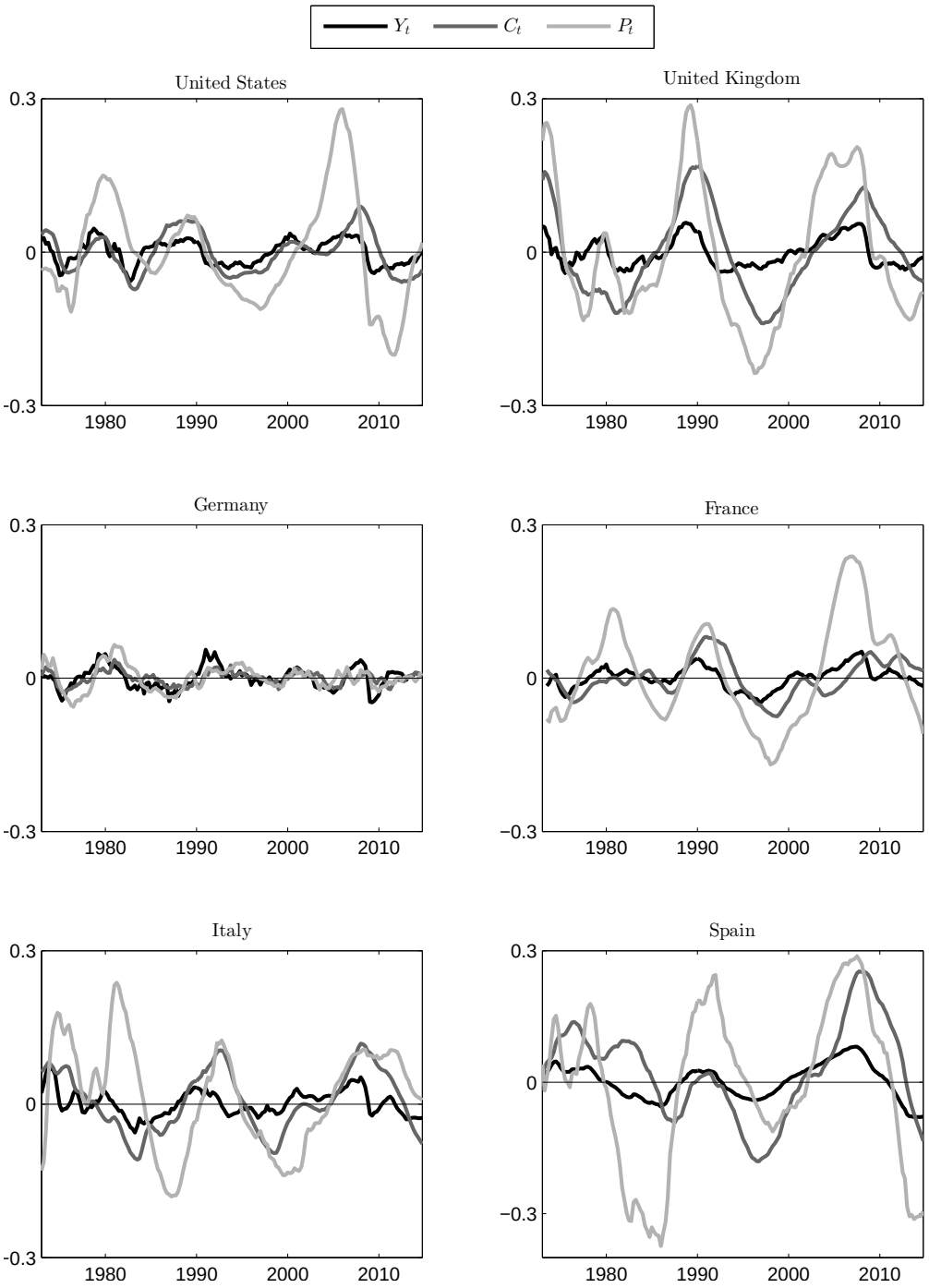

Note that the range of the y-axis differs for Spain.

Second, these cross-country differences correspond closely to shares of private home ownership in the individual countries. In between 1995 and 2013, the average shares stood at 85% in Spain, 76% in Italy, 72% in the U.K., 67% in the U.S., 64% in France, and 52% in Germany. As shown in Figure 2, a higher share of private home ownership corresponds to a higher average cycle length and standard deviation of credit volume and house price cycles.[9]

Third, we find the financial cycles to be closely related to the GDP cycles. Estimates of coherences of GDP with financial cycles range from 0.53 to 0.93, those between credit and house price cycles from 0.43 to 0.68 (see Table 2). There is no clear pattern across countries. Average phase shifts indicate a lag of credit cycles with respect to GDP cycles of 1.0 to 3.0 years, while GDP and house price cycles evolve roughly contemporaneously. Only for Italy the estimates would indicate a high lag of the house price cycle with respect to the GDP cycle.

Figure 2: Home Ownership Rate and Cyclical Characteristics

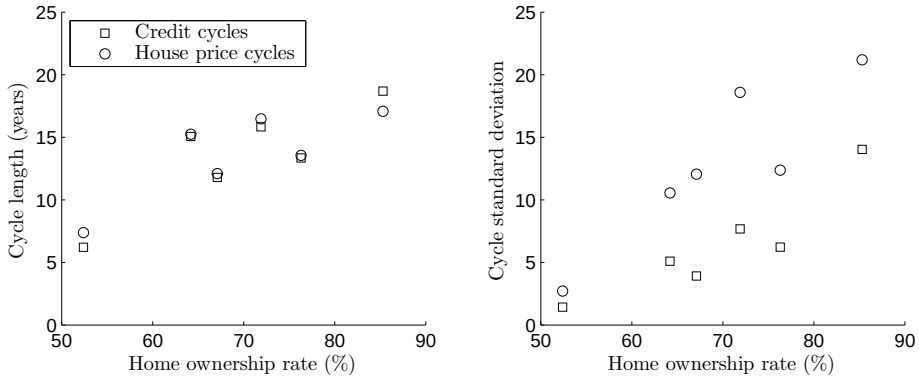

Fourth, estimating the GDP cycle jointly with financial series in a multivariate context also somewhat changes its characteristics. In particular, the estimates tend to emphasise a medium-term component in the GDP cycles that is not fully present in estimates from the univariate STSMs. Table 2 shows that estimates of average cycle lengths $2\pi/4\lambda^G$ from the multivariate STSM exceed those from the univariate STSM by 1.0 to 4.3 years. Moreover, the standard

[9]The data on private home ownership are taken from the FRED database for the U.S. and from Eurostat for the remaining countries. The Eurostat data starts in 1995.

deviations of cyclical components are by about 1 percentage point higher.

A closer inspection of the SGFs of cyclical components shows that it is mostly the fluctuations at the medium-term frequencies that account for the high coherences of GDP with the financial cycles. Table 3 shows that the average coherences among the cyclical components separately for the frequency bands of $32-120$ and $8-32$ quarters. We obtain these statistics from calculating the integrals in equation (9) over the respective subranges.[10] With the exception of Germany, the contribution of the longer frequency band to the overall variance is above 0.8 for the financial cycles and still higher than 0.7 for GDP cycles. Coherences are in general higher for the lower frequencies. The strong co-movement in the medium term is also evident in Figure 1, which documents three major peaks in financial cycles in the late 1970s, the early 1990s, and around 2007. GDP cycles are subject to shorter and more frequent fluctuations, but their major peaks and troughs correspond to those in the financial cycles.[11]

Table 3: Coherences at Different Frequency Bands

	U.S.	U.K.	DE	FR	IT	ES
Variance contribution $32-120$ quarters						
Y_t	.745	.878	.551	.894	.767	.961
C_t	.862	.935	.546	.939	.875	.974
P_t	.871	.948	.575	.942	.879	.954
Coherences $32-120$ quarters						
Y_t,C_t	.851	.540	.860	.931	.607	.840
Y_t,P_t	.774	.957	.664	.745	.848	.737
C_t,P_t	.526	.604	.733	.622	.453	.473
Coherences $8-32$ quarters						
Y_t,C_t	.699	.556	.685	.633	.423	.579
Y_t,P_t	.507	.578	.597	.616	.497	.833
C_t,P_t	.478	.563	.655	.463	.373	.258

The table shows the coherences between the cyclical components at frequency bands of 32-120 and 8-32 quarters, as well as the contribution of the 32-120 band to their overall variance. All statistics are calculated from the weighted integral presented in equation (9) over the respective bands.

[10] Figures A.7 toA.12 in Supplement A plot auto and cross spectra of cyclical components.

[11] see e.g. Breitung and Eickmeir (2014) and Miranda-Agrippino and Rey (2015) for studies on international co-movements in financial cycles.

Our estimates are not consistent with the notion that GDP cycles are represented by a frequency band of 8 to 32 quarters, as is commonly used in the application of band-pass filters. However, estimates from other sources do contain such medium-term components. Multivariate unobserved components models including real activity variables and inflation estimate the average length of the euro area business cycle at about 10 years (Proietti et al., 2007; Jarocinski and Lenza, 2015), while Comin and Gertler (2006) have documented medium-term business cycles in the U.S.

Table 4 shows that annual output gap measures from the OECD and the IMF are highly correlated with both estimates from the STSM and from the Christiano-Fitzgerald (CF) band-pass filter (Christiano and Fitzgerald, 2003) based on a frequency band of $32-120$ quarters. The correlations with the CF filter based on the $8-32$ quarter frequency band turn out to be considerably lower, again with the exception of Germany. Moreover, we find our estimates of financial cycles to be highly correlated with the CF-filter estimates from the $32-120$ quarter frequency band.[12]

Table 4: Sample Correlations between GDP Cycles, 1980-2014

		U.S.	U.K.	DE	FR	IT	ES
GDP							
IMF	STSM	.865	.909	.859	.567	.651	.890
	CF 32-120	.696	.818	.588	.697	.617	.827
	CF 8-32	.477	.311	.628	.415	.386	.280
OECD	STSM	.953	.888	.	.775	.808	.897
	CF 32-120	.881	.769	.	.810	.618	.801
	CF 8-32	.282	.491	.	.553	.375	.343
STSM	CF 32-120	.851	.920	.649	.824	.673	.950
	CF 8-32	.495	.344	.677	.327	.430	.124
IMF	OECD	.954	.858	.	.926	.650	.961

The table shows the annual sample correlations between cycles extracted by the STSM and CF filter and, for GDP, the IMF and OECD output gap measures. The latter two are available at annual frequencies from 1980 and 1985 onwards, respectively. OECD gap measures for Germany are only available after 1991.

[12] See Supplement B for graphs and sample cross-correlations between the CF filter estimates.

4 Properties of Pseudo Real-Time Estimates

Figure 1 shows full-sample estimates $\widehat{\mathbf{x}}^C_{t|T}$ of cyclical components. Economic policy, however, necessarily relies on estimates $\widehat{\mathbf{x}}^C_{t|t}$ from data sets $\mathcal{X}_t = \{\mathbf{x}_\tau\}^t_{\tau=1}$ that are available in real-time. So far, there is hardly any evidence on the reliability of real-time estimates of financial cycles, but various studies have investigated the issue for the output gap. Orphanides and van Norden (2001) report large differences in real-time estimates from different methods and conclude that output gap estimates are of limited value for policy purposes. Edge and Meisenzahl (2011) replicate the approach of Orphanides and van Norden (2001) for the U.S. credit-to-GDP ratio and reach equivalent conclusions. However, most of the methods included in these two studies, such as univariate filters and deterministic trends, arguably are of poor quality. Other studies on the output gap have shown that multivariate unobserved components models considerably improve upon univariate detrending methods, as they exploit the information contained in cyclical co-movement (Rünstler, 2002; Watson, 2007; Basistha and Startz, 2008; Trimbur, 2009).

In this section we provide some evidence on the properties of pseudo real-time estimates from the multivariate STSM. The purpose of our analysis is to assess the precision of estimates of financial cycles in comparison with the traditional business cycle by using the latter as a benchmark. We start with a Monte Carlo simulation and will then inspect the estimates from our empirical models.

4.1 Monte Carlo Simulation

The Monte Carlo simulation examines the precision of estimates of cyclical components under different assumptions on their size, length, and persistence. We use a bivariate model to study the gains from taking into account the information on cyclical co-movements.

We proceed as follows:

- We generate time series from a bivariate similar cycles model, $\mathbf{x}_t = \boldsymbol{\mu}_t + \mathbf{x}^C_t$, as given by equations (2), (5), and (8).

  We use three different simulation designs. The first two designs represent stylised versions of business (BC) and financial cycles (FC) dynamics, respectively. For simulation BC,

we assume a cycle length of 7 years and a standard deviation of cyclical components of $\sigma^C = 0.025$. The respective values for simulation FC are 15 years and $\sigma^C = 0.100$, close to our estimates for house prices in the U.S., France and Italy. Further, the standard deviations of trend innovations reflect our estimates on GDP and house prices from section 3.

Table 5: Monte Carlo Simulation Design

		ρ	$2\pi/4\lambda$	ϕ	σ^C	σ_η	σ_ζ
Business cycles	BC	.95	7.00	.000	2.500	.050	.050
Financial cycles	FC	.95	15.00	.800	10.000	.100	.100
Hybrid design	HC	.95	15.00	.800	2.500	.050	.050

The table shows the parameters of the three simulation designs.

The third, hybrid, design HC maintains the cycle length and persistence of simulation FC, but assumes standard deviations of cycles and trend innovations as in simulation BC. The purpose of the hybrid design is to disentangle the effects of the higher length and persistence of financial cycles (in comparison with BC) and their larger size (in comparison with FC).

The parameters of the simulation designs are shown in Table 5. In all three designs, we use the same parameters for both series. We abstract from phase shifts by setting $A^* = 0_{2\times 2}$ and choose matrix A to achieve the above values of σ^C together with a coherence of 0.7 between the two cyclical components.

- For each design, we generate 500 replications of data $\{\mathbf{x}_s\}_{s=1}^T$ with $T = 360$ observations from the bivariate STSM. To account for parameter uncertainty, we split each draw into two sub-samples: the first 180 observations are used to estimate model parameters by maximum likelihood; we then obtain estimates of cyclical components from the remaining observations. Given that the dynamics of the two series in the bivariate model are identical, it is sufficient to inspect the estimates for the first series. To obtain the corresponding estimates from the univariate STSM and the CF filter, we simply apply these methods to the first series. For the CF filter we use frequency bands of $8 - 32$ quarters for simulation BC and $32 - 120$ quarters for simulations FC and HC.

We inspect estimates of the cyclical component in series 1, $\widehat{x}^C_{1,t|t+h}$, based on information sets $\mathcal{X}_{t+h} = \{\mathbf{x}_s\}_{s=181}^{t+h}$ for different values of h. For instance, estimates $\widehat{x}^C_{1,t|t}$ represent real-time estimates, while smoothed estimates $\widehat{x}^C_{1,t|t+20}$ would use information up to 20 quarters ahead. The latter estimates are very close to the full-sample estimates $\widehat{x}^C_{1,t|T}$, while providing a more consistent benchmark for the real-time estimates.

The simulation outcomes are shown in Table 6. We assess the precision of estimates $\widehat{x}^C_{1,t|t+h}$ from the root mean square error (RMSE) with respect to the generated cycles $x^C_{1,t}$. Table 6 shows this statistic together with the standard deviations of estimates $\widehat{x}^C_{1,t|t+h}$. Both are shown relative to the standard deviation of the generated cycles, σ^C.

Table 6: Monte Carlo Simulation Results

	Standard deviations			RMSE		
	$h=0$	$h=4$	$h=20$	$h=0$	$h=4$	$h=20$
Business cycles (BC)						
STSM bivariate	.791	.871	.916	.700	.582	.450
STSM univariate	.748	.821	.852	.769	.652	.530
CF filter (8 - 32)	.542	.680	.800	.819	.673	.612
Financial cycles (FC)						
STSM bivariate	.711	.786	.877	.775	.701	.518
STSM univariate	.717	.794	.893	.819	.740	.556
CF filter (32 - 120)	.538	.566	.901	.802	.780	.584
Hybrid design (HC)						
STSM bivariate	.665	.730	.811	.939	.872	.720
STSM univariate	.651	.716	.781	.998	.935	.798
CF filter (32 - 120)	.714	.732	1.059	.936	.912	.818

The table shows the sample standard deviations and RMSE of $\widehat{x}^C_{1,t|t+h}$ with respect to the generated values, $x^C_{1,t}$ for different values of h. All values are shown relative to the standard deviation of the generated cycles, σ^C.

For the bivariate STSM, we find the relative RMSE of real-time estimates $\widehat{x}^C_{1,t|t}$ to be moderately higher for simulation FC than for BC. This emerges as a net result of two opposing effects related to cycle lengths and signal-noise ratios. First, the higher length and persistence of cycles in simulation HC compared to BC results in a substantially larger relative RMSE. Second, simulation

design *FC* implies a more favourable signal-to-noise ratio than *HC*, i.e. larger cyclical components relative to the volatility of trends. This acts to reduce the RMSE. Taken together, the relative RMSE of real-time estimates amounts to 0.78 for simulation *FC*, compared to 0.70 for *BC*. Once h increases, the relative RMSEs of estimates decline. For $h = 20$ they become 0.45 for *BC* and 0.52 for *FC*. Correspondingly, standard deviations of cyclical estimates get closer to the true standard deviation σ^C as h increases.

For simulations *BC* and *FC* the bivariate STSM provides consistently better real-time estimates than the univariate STSM and the CF filter. The relative RMSE is always smaller, although the gains are somewhat smaller for simulation *FC*. In addition, the CF filter grossly underestimates the standard deviations of the cycles in real-time. For simulation *HC* the CF filter performs equally well, as the parameter estimates in the STSM are subject to larger standard errors.

4.2 Empirical Pseudo-Real Time Estimates

We turn to the inspection of pseudo real-time estimates of cycles $\widehat{\mathbf{x}}^C_{t|t}$ for the countries in our sample. Following earlier studies (e.g. Orphanides and van Norden, 2002), we examine the revisions of real-time to smoothed estimates $\widehat{\mathbf{x}}^C_{t|t} - \widehat{\mathbf{x}}^C_{t|t+20}$. As the smoothed estimates are more precise than the real-time estimates, the size of the revisions gives an indication of the relative performance of the models. Figure 3 plots both estimates for the various cyclical components. Table 7 reports the sample standard deviations of the real-time estimates and the RMSE of revisions relative to the sample standard deviation of the smoothed estimates $\widehat{\mathbf{x}}^C_{t|t+20}$. In contrast to the results reported in section 4.1, the graphs and statistics are based on full-sample estimates of model parameters and therefore do not take into account parameter instability.[13]

Overall, our findings for the multivariate STSM are similar to the above simulation results. In most cases, the sample standard deviations of real-time estimates $\widehat{x}^C_{i,t|t}$ are again close to 70% of those of the smoothed estimates $\widehat{x}^C_{i,t|t+20}$. Excluding Germany, the relative RMSE of revisions ranges from 0.38 to 0.62 for house price, 0.45 to 0.68 for credit and 0.54 to 0.67 for GDP cycles.

[13] Our sample of 45 years contains only three full financial cycles and is therefore arguably too short for the recursive estimation of model parameters.

Figure 3: Real-Time Estimates of Cyclical Components

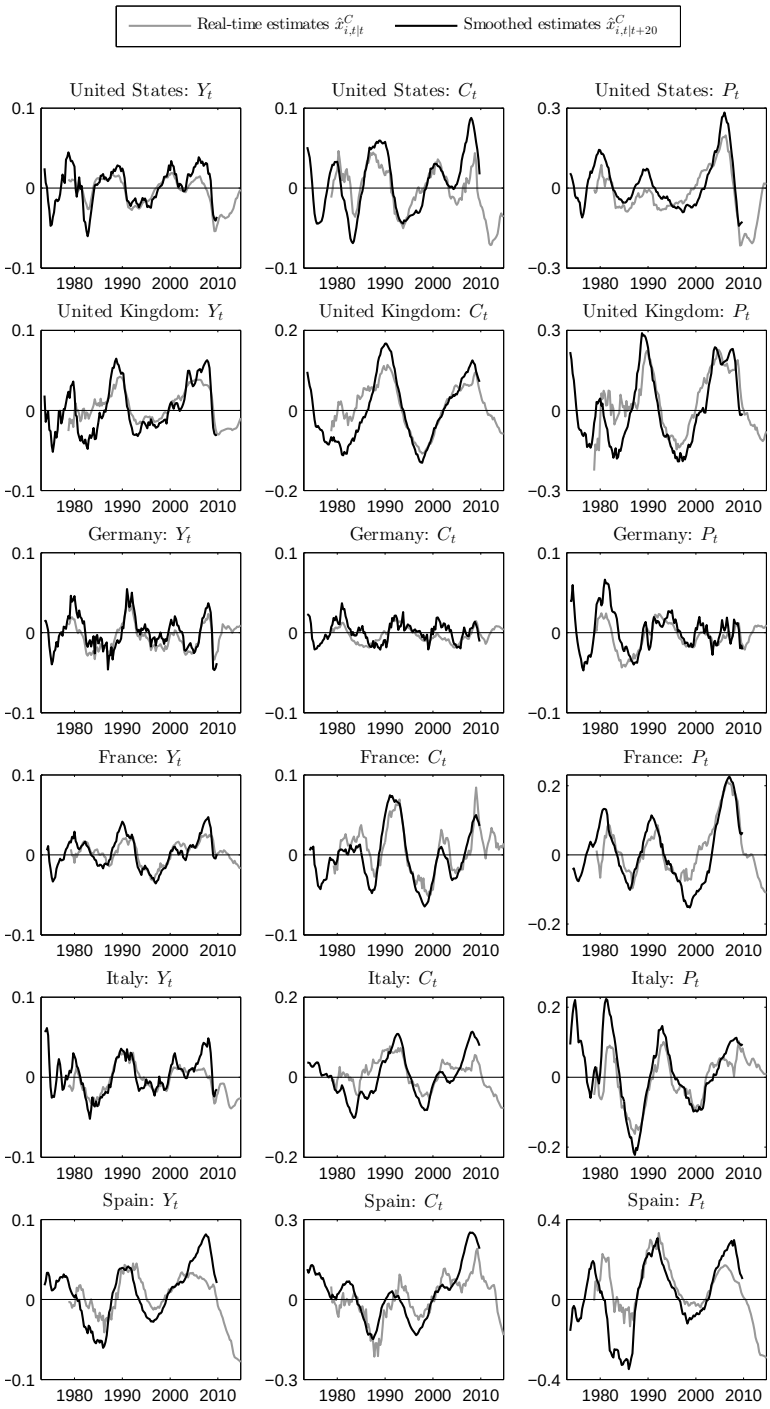

Hence, conditional on the parameter estimates, real-time estimates of house price cycles appear somewhat more reliable than those of GDP and credit cycles. Our simulation results suggest that this can be attributed to the larger standard deviation of house price cycles. For Germany, the size of revisions is relatively large given the small size of the cyclical components.

Table 7: Properties of Real-Time Estimates

	GDP		Credit		House prices	
	Std	RMSE	Std	RMSE	Std	RMSE
Multivariate STSM						
U.S.	.735	.558	.620	.683	.887	.502
U.K.	.593	.542	.744	.448	.718	.507
Germany	.855	.445	.894	.823	.913	.770
France	.736	.526	.846	.484	.807	.467
Italy	.750	.561	.573	.690	.742	.386
Spain	.548	.673	.775	.629	.574	.624
Christiano-Fitzgerald filter						
U.S.	.747	.657	.418	.693	.447	.637
U.K.	.843	.825	.629	.682	.475	.617
Germany	.595	.621	.700	.829	.831	.640
France	.758	.800	.539	.627	.568	.571
Italy	.714	.655	.523	.658	.533	.560
Spain	.986	1.018	.591	.730	.424	.624

Columns Std and RMSE show the sample standard deviations of $\widehat{\mathbf{x}}^C_{t|t}$ and the RMSE of revisions of $\widehat{\mathbf{x}}^C_{t|t}$ with respect to $\widehat{\mathbf{x}}^C_{t|t+20}$. All values are shown relative to the sample standard deviations of $\widehat{\mathbf{x}}^C_{t|t+20}$.

Further, Table 7 confirms the better performance of the multivariate STSM compared to the CF filter. Again, we use frequency bands of $8-32$ quarters for GDP and $32-120$ quarters for the financial series. For all three series, the relative RMSE of revisions is almost always smaller for the multivariate STSM. In addition, for the financial cycles the downward bias in the standard deviations of real-times estimates is almost always smaller. While the latter finding does not hold for GDP cycles, the results are not directly comparable, as the CF filter bands imply shorter cycles than the STSM estimates.

5 Conclusions

The purpose of this paper was to estimate financial cycles for the U.S. and the five largest European economies, and to study their relationships with business cycles. For this purpose, we developed a version of the multivariate STSM that allows for the joint modelling of business and financial cycles and accounts for the high persistence in the latter.

In line with other studies, we found large and persistent cycles in real credit volumes and real house prices with a length of about 15 years. The only exception is Germany, where financial cycles are characterised by relatively small short-term fluctuations.

We also found a close association between financial cycles and a medium-term component in the GDP cycle. While earlier studies have already noted that troughs in financial cycles coincide with particularly deep recessions (Drehmann et al, 2012; Claessens et al., 2012), our estimates indicate a more systematic relationship between financial cycles and GDP at medium-term frequencies over the entire cycle. This suggests possible gains from the coordination of monetary and macro-prudential policies.

Another finding of the paper is that the differences in cyclical characteristics across countries are closely related to private home ownership rates: financial cycles are larger and longer for countries with high home ownership rates. Given our small sample of six countries, these findings are only indicative. They therefore may warrant further research, as such cross-country differences might provide insights into the interaction of business and financial cycles and the role for country-specific macro-prudential policies in the euro area.

Finally, issues pertaining to the reliability of real-time estimates of financial cycles may be of no larger scale than those for the traditional business cycles: we find that the uncertainty of our real-time estimates of financial and GDP cycles, relative to their size, is roughly comparable. Furthermore, in line with earlier studies on the business cycle, our results confirm that multivariate model-based filters provide more precise real-time estimates than univariate model-based and non-parametric filters.

References

Aikman, D., A. Haldane and B. Nelson, 2015. Curbing the credit cycle, *The Economic Journal* **125**: 1072-1109.

Alessi, L. and C. Detken, 2014. Identifying excessive credit growth and leverage, ECB Working Paper No. 1723.

Basistha, A. and R. Startz, 2007. Measuring the NAIRU with reduced uncertainty: a multiple indicator-common cycle approach, *Review of Economics and Statistics* **90**(4): 805-811.

Breitung, J. and S. Eickmeir, 2014. Analyzing business and financial cycles using multi-level factor models, Deutsche Bundesbank Discussion Paper No. 11/2014.

Cerutti, I., S. Claessens, and L. Laeven, 2015. The use and effectiveness of macroprudential policies: new evidence, IMF Working Paper No.15/61.

Chen, X., A. Kontonikas and A. Montagnoli, 2012. Asset prices, credit and the business cycle, *Economic letters* **117**: 857-861.

Christiano, L.J. and T.J. Fitzgerald, 2003. The band pass filter, *International Economic Review* **44**(2): 435-465.

Claessens, S., M. Kose and M. Terrones, 2011. Financial cycles: what? how? when?, IMF Working Paper No. 11/88.

Claessens, S., M. Kose and M. Terrones, 2012. How do business and financial cycles interact?, *Journal of International Economics* **87**(1): 178-190.

Comin, D. and M. Gertler, 2006. Medium-term business cycles, *American Economic Review* **96**(3): 523-551.

De Bonis, R. and A. Silvestrini, 2013. The Italian financial cycle: 1861-2011, Banca d'Italia Working Paper No. 936.

Drehmann, M., C. Borio and K. Tstsaronis, 2012. Characterising the financial cycle: don't lose sight of the medium term!, BIS Working Paper No. 380.

Durbin, J. and S.J. Koopman, 2001. *Time Series Analyis by State Space Methods*, Oxford: Oxford University Press.

ECB, 2008. *The incentive structure of the 'originate and distribute' model*, European Central Bank.

Edge, R. and R. Meisenzahl, 2011. The unreliability of credit-to-GDP ratio gaps in real time: implications for counter-cyclical capital buffers, *International Journal of Central Banking* **7**(4): 261:298.

Galati, G., S.J. Koopman, I. Hindrayanto and M. Vlekke. 2015, Extracting financial cycles with a model-based filter: evidence from the United States and the Euro Area, Dutch National Bank, mimeo.

Geanakoplos J., 2009. The leverage cycle, in D.Acemoglu, K. Rogoff and M. Woodford (eds.), *NBER Macroeconomics Annual Vol. 24*, University of Chicago Press.

Giese, J., H. Andersen, O. Bush, C. Castro, M. Farag and S. Kapadia, 2014. The credit-to-GDP gap and complementary indicators for macro-prudential policy: evidence from the U.K., *International Journal of Finance and Economics* **19**(1): 25-47.

Hamilton, J., 1994. *Time Series Analysis*, Princeton: Princeton University Press.

Harvey, A.C. and T. Trimbur, 2004. General model-based filters for extracting cycles and trends in economics time series, *The Review of Economics and Statistics* **85**(2): 244-255.

Harvey, A.C. and A. Jäger, 1993. Detrending, stylised facts, and the business cycle, *Journal of Applied Econometrics* **8**: 231-247.

Harvey, A.C. and S.J. Koopman, 1997. Multivariate structural time series models in C. Heij et al. (eds.), *System*

Dynamics in Economic and Financial Models, New York: John Wiley.

Jarocinski M. and M. Lenza, 2015. Output gap and inflation forecasts in a Bayesian dynamic factor model of the euro area, European Central Bank, mimeo.

Jordà, Ò., M. Schularick, and A. Taylor, 2014. The great mortgaging: housing finance, crises, and business cycles, NBER Working Paper No. 20501.

King R. and M. Watson, 1996. Money, Prices, Interest Rates and the Business Cycle, *The Review of Economics and Statistics* **78**(1): 35-53.

Koopman, S.J. and J. Valle e Azevedo, 2008. Measuring synchronization and convergence of business cycles for the euro area, U.K. and U.S., *Oxford Bulletin of Economics and Statistics* **70**(1): 23-51.

Orphanides, A. and S. Van Norden, 2002. The unreliability of output gap estimates in real-time. *Review of Economics and Statistics* **84**(4): 569-83.

Miranda-Agrippino, S. and H. Rey, 2015. World asset markets and the global financial cycle, mimeo.

Moës, P., 2012. Multivariate models with dual cycles: implications for output gap and potential growth measurement, *Empirical Economics* **42**(3): 791-818.

Proietti, T., A. Musso, T. Westermann, 2007. Estimating potential output and the output gap for the euro area: a model-based production function approach, *Empirical Economics* **33**(1): 85-113.

Rünstler G., 2002. The information content of real-time output gap estimates: an application to the Euro area, ECB Working Paper Series No. 182.

Rünstler G., 2004. Modelling phase shifts among stochastic cycles, *Econometrics Journal* **7**(1): 232-248.

Scatigna, M. R., Szemere, and K. Tsatsaronis, 2014. Residential property price statistics across the globe, BIS Quarterly Review, September 2014.

Schüler, Y., P. Hiebert and T. A. Peltonen, 2015. Characterising financial cycles across Europe: one size does not fit all, ECB Working Paper, ECB working paper 1846.

Trimbur, T., 2009. Improving real-time estimates of the output gap, Finance and Economics Discussion Series 2009-32, Federal Reserve Board.

Valle e Azevedo, J., S.J. Koopman and A. Rua, 2006. Tracking the business cycle of the euro area: a multivariate model-based bandpass filter, *Journal of Business and Economic Statistics* **24**(3): 278-290.

Watson, M., 2007. How accurate are real-time estimates of output trends and gaps? *Federal Reserve Bank of Richmond Economic Quarterly* **93**(2): 143-61.

Annex A: Properties of Stochastic Cycles

Autocovariance Generating Function under Similar Cycles

The annex adapts the proofs of Rünstler (2004) to the case of the extended stochastic cycle (SCE). We consider the $2n \times 1$ vector $\widetilde{\boldsymbol{\psi}}_t = (\boldsymbol{\psi}_t', \boldsymbol{\psi}_t^{*\prime})'$. The elements $\widetilde{\boldsymbol{\psi}}_{i,t} = \left(\psi_{i,t}, \psi_{i,t}^*\right)$ of $\widetilde{\boldsymbol{\psi}}_t$ follow stochastic processes as defined in equation (8) with covariance matrix $\mathbb{E}\left[\widetilde{\boldsymbol{\kappa}}_t \widetilde{\boldsymbol{\kappa}}_t{}'\right] = I_{2n}$.

Under the similar cycles restriction, the ACF of $\widetilde{\boldsymbol{\psi}}_t$ is given by

$$\widetilde{V}(s) = f(s;\rho,\phi)\left[T_1^+(s\lambda) \otimes I_n\right]$$

with scalar function $f(s;\rho,\phi) = [1-\phi s]\left[1-\phi s^{-1}\right] h(s;\rho)$ with $h(s;\rho)$ defined as in equation (4) in the main text. Note that $T^+(s\lambda) = T\cos(s\lambda) + T^*\sin(s\lambda)$, where

$$T = \begin{bmatrix} 1 & 0 \\ 0 & 1 \end{bmatrix}, \quad T^* = \begin{bmatrix} 0 & 1 \\ -1 & 0 \end{bmatrix}.$$

Denoting $\widetilde{A} = (A, A^*)$, the ACF of cyclical components $\mathbf{x}_t^C$ is then given by

$$V^C(s) = f(s;\rho,\phi)\left[B\cos(s\lambda) + B^*\sin(s\lambda)\right]$$

with symmetric $B = \widetilde{A}(T \otimes I_n)\widetilde{A}'$ and skew-symmetric $B^* = \widetilde{A}(T^* \otimes I_n)\widetilde{A}'$. From a polar transformation, the elements of B and B^* can be expressed as $b_{ij} = r_{ij}\cos(\lambda\theta_{ij})$ and $b_{ij}^* = r_{ij}\sin(\lambda\theta_{ij})$, respectively, with r_{ij} and θ_{ij} defined as in the main text. Using the trigonometric identity $\cos(\lambda\theta_{ij})\cos(\lambda s) + \sin(\lambda\theta_{ij})\sin(\lambda s) = \cos(\lambda(s-\theta_{ij}))$ the elements of the ACF $V^C(s)$ of $\mathbf{x}_t^C$ can finally be expressed as

$$V_{ij}^C(s) = f(s;\rho,\phi) r_{ij}\cos(\lambda(s-\theta_{ij}))\,.$$

The properties $b_{ij} = b_{ji}$ and $b_{ij}^* = -b_{ji}^*$ together with $\tan^{-1}(-x) = -\tan^{-1}(x)$ imply $\theta_{ji} = -\theta_{ij}$ and $r_{ij} = r_{ji}$.

The proofs of the identifying restrictions to be imposed on matrices (A, A^*) in the case of similar cycles carry over directly to the SCE, as replacing scalar function $h(s;\rho)$ with $f(s;\rho,\phi)$ does not change the argument. We use the Cholesky decomposition proposed by Rünstler (2004). The case of non-similar cycles evidently does not require lower triangularity of A and A^* to achieve identifiability. However, the restrictions $a_{ii}^* = 0$ for $i = 1,\ldots,n$ are required, as phase shifts are identified only in relative terms. In case that subsets of m SCEs share similar dynamics, Cholesky decompositions are applied to the respective $n \times m$ submatrices of A and A^*.

Spectral Generating Function

Denote the spectral generating function (SGF) of the SCE $\widetilde{\psi}_{i,t}$ with

$$\widetilde{G}_{ii}(\omega) = \sigma_{\kappa,ii}^2 \begin{bmatrix} g_1(\omega) & g_{12}(\omega) \\ g_{12}^H(\omega) & g_2(\omega) \end{bmatrix},$$

where $g^H(.)$ denotes the complex conjugate of $g(.)$. The properties of $\widetilde{V}_{ii}(s)$ imply that $g_1(\omega) = g_2(\omega)$ and that the real part of the cross spectrum is zero. The SGF of the extended SC as in equation (8) is given by

$$\begin{aligned} g_1(\omega) &= \frac{1+\rho^2-2\rho\cos\lambda\cos\omega}{D} g_A(\omega)\,, \\ g_{12}(\omega) &= -\mathbf{i}\frac{2\rho\sin\lambda\sin\omega}{D} g_A(\omega)\,, \\ g_A(\omega) &= \left(1+\phi^2-2\phi\cos\omega\right)^{-1}, \end{aligned}$$

where $D = \left[1+\rho^4+2\rho^2-4\rho(1+\rho^2)\cos\lambda\cos\omega+2\rho^2(\cos 2\lambda+\cos 2\omega)\right]$ and $g_A(\omega)$ is the SGF of an AR(1).

In the case of similar cycles, the SGF $G^C(\omega) = \widetilde{A}\left[\widetilde{G}_{ii}(\omega) \otimes I_n\right]\widetilde{A}'$ of cyclical components $\mathbf{x}_t^C$ can be expressed as

$$G^C(\omega) = Bg_1(\omega) + B^* g_{12}(\omega) \; .$$

In the case of non-similar cycles, closed-form expressions for $G^C(\omega)$ do no longer exist. It is most conveniently calculated from the general expressions for stationary stochastic processes. The SGF $G(\omega)$ of a multivariate stationary stochastic process $\mathbf{v}_t = \Psi(L)\mathbf{e}_t$ with $\mathbb{E}\mathbf{e}_t\mathbf{e}_t' = \Sigma_e$ is given by

$$G(\omega) = [\Psi(\exp(-\mathbf{i}\omega))]\,\Sigma_e\,[\Psi(\exp(-\mathbf{i}\omega))]'$$

for $-\pi \leq \omega \leq \pi$ (see e.g. Hamilton 1994:267f). We use this expression to obtain the joint SGF $G(\omega)$ of vector $\widetilde{\psi}_t$ from the stationary part of the transition equation of the state space form and calculate the SGF of cyclical components $\mathbf{x}_t^C$ from $G^C(\omega) = (A, A^*)G(\omega)(A, A^*)'$. Coherence and phase spectra are found from the general expressions (Hamilton, 1994:275f). We finally obtain average cycle lengths, coherences and phase shifts, as reported in Tables 2 and 3, from equation (9).

Business and Financial Cycles:

an Unobserved Components Model Perspective

Gerhard Rünstler and Marente Vlekke

European Central Bank

October 2015

SUPPLEMENTS FOR ONLINE PUBLICATION

Supplement A: Tables and Figures of the Three Main Models

A1. Tables Description

Tables A.1 to A.6 show the estimation results for the univariate and the restricted and unrestricted multivariate models. More precisely, estimates for the univariate model and the multivariate model in column 2 are obtained under the restriction that the standard deviations of the slope innovations of C_t and P_t equal 0.001. For credit volumes in Spain we use a value of 0.0025. Column 3 shows the results for unrestricted slope estimates. All three models impose similar cycle restrictions on C_t and P_t. $2\pi/4\lambda$ denotes the estimated cycle length of the stochastic cycles $\psi_{i,t}$ in years. The third panel shows stylised facts on cyclical co-movements derived from the SGF (see section 2.2 and annex A). The upper part of the panel shows estimated average cycle lengths in years ($2\pi/4\lambda^G$) and standard deviations σ^C, while the lower part shows coherences (lower left) and phase shifts in years (upper right) between the cyclical components. LL and R_D^2 refer to the log-likelihood and the coefficient of determination with respect to the first difference of the series, respectively. The Ljung-Box statistic $Q(20)$ tests for autocorrelation in standardized prediction errors based on 20 lags, and follows a $\chi^2(20)$ distribution. LR statistic a) tests for extended cyclical dynamics (see equation (8)). Statistics b) and c) test for similar cyclical dynamics in all three series and between C_t and P_t, respectively (see section 3.1 for details). * and ** denote statistical signifiance at the 5% and 1% level, respectively.

A2. Figures Description

Figures A.1-A.6 show the smoothed estimates from the multivariate STSM with restricted slopes, as presented in the main text. The first and second row show the data and trend, and the data and level of the trend in first differences, respectively. The second row also shows the slope. The third row shows the corresponding smoothed cycle, while the fourth row shows the standardized prediction errors. The final row shows the output of the Christiano-Fitzgerald filter for a frequency band of 8-32 quarters for GDP and 32-120 quarters for credit and house prices.

Figures A.7-A.12 show the spectral generating functions of the cyclical components of the three series. The diagonal figures show auto spectra. The lower-left off-diagonal figures show coherences between the cyclical components, as derived from the SGF, while the upper-right off-diagonal figures show phase spectra. A positive value of the phase stands for a lead of series row to series column.

Table A.1: Main Parameter Estimates United States

	Univariate			Multivariate Restricted slopes			Multivariate Estimated slopes		
1. Trend parameters									
	Y_t	C_t	P_t	Y_t	C_t	P_t	Y_t	C_t	P_t
$\sigma_\eta \times 100$	0.533	0.244	0.001	0.000	0.000	0.000	0.000	0.000	0.000
$\sigma_\zeta \times 100$	0.037	0.100	0.100	0.031	0.100	0.100	0.030	0.042	0.014
2. Parameters stochastic cycles									
	$\psi_{1,t}$	$\psi_{2,t}$		$\psi_{1,t}$	$\psi_{2,t}$		$\psi_{1,t}$	$\psi_{2,t}$	
ϕ	0.483	0.920		0.000	0.859		0.000	0.865	
ρ	0.935	0.945		0.860	0.956		0.896	0.967	
$2\pi/4\lambda$	8.995	12.514		4.770	10.795		5.466	13.909	
3. Cyclical components									
	Y_t	C_t	P_t	Y_t	C_t	P_t	Y_t	C_t	P_t
$2\pi/4\lambda^G$	7.718	16.551	16.551	8.735	11.792	12.105	9.469	14.593	14.888
$\sigma^C \times 100$	2.119	5.616	16.734	2.535	3.913	12.053	2.615	5.570	15.965
					Phase			Phase	
				Y_t^C	C_t^C	P_t^C	Y_t^C	C_t^C	P_t^C
			Y_t^C		1.432	0.575		1.872	1.172
		Coherence	C_t^C	0.805		-1.409	0.743		-1.536
			P_t^C	0.726	0.509		0.744	0.529	
4. Diagnostics									
	Y_t	C_t	P_t	Y_t	C_t	P_t	Y_t	C_t	P_t
LL			2265.140			2291.795			2292.136
R_D^2	0.105	0.784	0.767	0.215	0.809	0.760	0.209	0.812	0.761
$Q(20)$	27.810	21.325	28.456	28.036	26.851	28.988	30.289	25.719	28.278
5. Likelihood ratio tests									
a) $\phi_1 = \phi_2 = \phi_3 = 0$			**135.360						
b) Similar Cycles (Y, C, P)			10.300						
c) Similar Cycles (C, P)			4.594						

For notation see section A1. We used one dummy to account for a level shift in credit in 1980Q1. For house prices, we used two dummies to account for an additive outlier in 1976Q3 and a level shift in 1976Q4, respectively.

Table A.2: Main Parameter Estimates United Kingdom

	Univariate			Multivariate Restricted slopes			Multivariate Estimated slopes		
1. Trend parameters									
	Y_t	C_t	P_t	Y_t	C_t	P_t	Y_t	C_t	P_t
$\sigma_\eta \times 100$	0.000	1.627	1.269	0.000	1.556	1.183	0.020	1.567	1.217
$\sigma_\zeta \times 100$	0.049	0.100	0.100	0.035	0.100	0.100	0.019	0.114	0.037
2. Parameters stochastic cycles									
	$\psi_{1,t}$	$\psi_{2,t}$		$\psi_{1,t}$	$\psi_{2,t}$		$\psi_{1,t}$	$\psi_{2,t}$	
ϕ	0.286	0.720		0.000	0.693		0.000	0.727	
ρ	0.953	0.982		0.931	0.979		0.932	0.980	
$2\pi/4\lambda$	12.729	18.119		8.192	18.535		8.141	18.856	
3. Cyclical components									
	Y_t	C_t	P_t	Y_t	C_t	P_t	Y_t	C_t	P_t
$2\pi/4\lambda^G$	9.527	16.754	16.754	13.487	15.837	16.476	14.385	16.459	17.168
$\sigma^C \times 100$	2.976	9.220	21.514	4.094	7.6832	18.593	4.578	7.988	21.110
					Phase			Phase	
				Y_t^C	C_t^C	P_t^C	Y_t^C	C_t^C	P_t^C
			Y_t^C		1.976	0.739		1.864	0.797
		Coherence	C_t^C	0.532		-1.274	0.573		-1.137
			P_t^C	0.927	0.598		0.941	0.638	
4. Diagnostics									
	Y_t	C_t	P_t	Y_t	C_t	P_t	Y_t	C_t	P_t
LL			1873.874			1898.631			1899.585
R_D^2	0.183	0.224	0.397	0.236	0.249	0.404	0.242	0.252	0.405
$Q(20)$	18.512	17.807	19.834	22.221	17.003	20.650	22.969	16.501	21.295
5. Likelihood ratio tests									
a) $\phi_1 = \phi_2 = \phi_3 = 0$				**31.970					
b) Similar Cycles (Y, C, P)				9.187					
c) Similar Cycles (C, P)				0.371					

For notation see section A1.

Table A.3: Main Parameter Estimates Germany

	Univariate			Multivariate Restricted slopes			Multivariate Estimated slopes		
1. Trend parameters									
	Y_t	C_t	P_t	Y_t	C_t	P_t	Y_t	C_t	P_t
$\sigma_\eta \times 100$	0.730	0.517	0.002	0.000	0.000	0.000	0.000	0.000	0.000
$\sigma_\zeta \times 100$	0.021	0.100	0.100	0.036	0.100	0.100	0.030	0.100	0.065
2. Parameters stochastic cycles									
	$\psi_{1,t}$	$\psi_{2,t}$		$\psi_{1,t}$	$\psi_{2,t}$		$\psi_{1,t}$	$\psi_{2,t}$	
ϕ	0.000	0.147		0.000	0.262		0.000	0.336	
ρ	0.944	0.941		0.630	0.936		0.596	0.931	
$2\pi/4\lambda$	5.822	11.642		5.427	9.317		4.221	9.810	
3. Cyclical components									
	Y_t	C_t	P_t	Y_t	C_t	P_t	Y_t	C_t	P_t
$2\pi/4\lambda^G$	5.135	8.172	8.172	6.336	6.193	7.112	6.554	6.414	7.424
$\sigma^C \times 100$	1.360	1.215	2.774	2.147	1.431	2.712	2.225	1.477	2.966
				Phase			Phase		
				Y_t^C	C_t^C	P_t^C	Y_t^C	C_t^C	P_t^C
			Y_t^C		1.076	1.132		1.396	1.418
		Coherence	C_t^C	0.740		0.158	0.737		0.076
			P_t^C	0.610	0.683		0.615	0.708	
4. Diagnostics									
	Y_t	C_t	P_t	Y_t	C_t	P_t	Y_t	C_t	P_t
LL			2129.141			2148.373			2148.453
R_D^2	0.032	0.339	0.061	0.130	0.345	0.097	0.133	0.348	0.094
$Q(20)$	*31.960	21.252	*35.886	*35.715	21.721	30.509	*35.250	21.517	29.917
5. Likelihood ratio tests									
a) $\phi_1 = \phi_2 = \phi_3 = 0$				1.764					
b) Similar Cycles (Y, C, P)				3.098					
c) Similar Cycles (C, P)				0.67					

For notation see section A1. We used one dummy for credit to account for a level shift in 1994Q4.

Table A.4: Main Parameter Estimates France

	Univariate			Multivariate Restricted slopes			Multivariate Estimated slopes		
1. Trend parameters									
	Y_t	C_t	P_t	Y_t	C_t	P_t	Y_t	C_t	P_t
$\sigma_\eta \times 100$	0.292	0.502	0.304	0.079	0.470	0.289	0.202	0.499	0.313
$\sigma_\zeta \times 100$	0.031	0.100	0.100	0.054	0.100	0.100	0.022	0.000	0.060
2. Parameters stochastic cycles									
	$\psi_{1,t}$	$\psi_{2,t}$		$\psi_{1,t}$	$\psi_{2,t}$		$\psi_{1,t}$	$\psi_{2,t}$	
ϕ	0.850	0.850		0.000	0.821		0.000	0.939	
ρ	0.822	0.951		0.892	0.969		0.917	0.927	
$2\pi/4\lambda$	5.895	16.672		3.187	15.407		3.000	10.993	
3. Cyclical components									
	Y_t	C_t	P_t	Y_t	C_t	P_t	Y_t	C_t	P_t
$2\pi/4\lambda^G$	8.584	16.509	16.509	12.572	15.057	15.250	13.912	17.312	17.553
$\sigma^C \times 100$	1.692	4.917	9.900	2.678	5.099	10.551	2.559	4.794	10.930
					Phase			Phase	
				Y_t^C	C_t^C	P_t^C	Y_t^C	C_t^C	P_t^C
			Y_t^C		2.669	-0.705		2.230	-0.272
		Coherence	C_t^C	0.875		-4.455	0.759		-3.989
			P_t^C	0.734	0.572		0.690	0.355	
4. Diagnostics									
	Y_t	C_t	P_t	Y_t	C_t	P_t	Y_t	C_t	P_t
LL			2258.341			2291.226			2294.333
R_D^2	0.367	0.368	0.785	0.405	0.466	0.788	0.431	0.469	0.787
$Q(20)$	21.567	24.959	23.092	22.752	29.749	22.532	23.965	28.302	23.680
5. Likelihood ratio tests									
a) $\phi_1 = \phi_2 = \phi_3 = 0$				**97.908					
b) Similar Cycles (Y, C, P)				10.292					
c) Similar Cycles (C, P)				1.809					

For notation see section A1. We used one dummy to account for a level shift in GDP in 1975Q3, and three dummies for credit to account for level shifts in 1975Q3, 1978Q2 and 1986Q4. We used one dummy to account for an additive outlier in house prices in 1997Q1.

Table A.5: Main Parameter Estimates Italy

	Univariate			Multivariate Restricted slopes			Multivariate Estimated slopes		
1. Trend parameters									
	Y_t	C_t	P_t	Y_t	C_t	P_t	Y_t	C_t	P_t
$\sigma_\eta \times 100$	0.449	0.906	0.000	0.052	0.876	0.208	0.039	0.926	0.206
$\sigma_\zeta \times 100$	0.050	0.100	0.100	0.057	0.100	0.100	0.053	0.222	0.077
2. Parameters stochastic cycles									
	$\psi_{1,t}$	$\psi_{2,t}$		$\psi_{1,t}$	$\psi_{2,t}$		$\psi_{1,t}$	$\psi_{2,t}$	
ϕ	0.886	0.726		0.000	0.726		0.000	0.763	
ρ	0.848	0.967		0.912	0.955		0.907	0.918	
$2\pi/4\lambda$	3.124	19.255		2.972	15.578		2.926	9.845	
3. Cyclical components									
	Y_t	C_t	P_t	Y_t	C_t	P_t	Y_t	C_t	P_t
$2\pi/4\lambda^G$	5.931	16.359	16.359	9.240	13.354	13.553	6.712	9.588	9.821
$\sigma^C \times 100$	1.917	7.517	15.588	2.918	6.220	12.37	2.302	3.485	9.330
					Phase			Phase	
				Y_t^C	C_t^C	P_t^C	Y_t^C	C_t^C	P_t^C
			Y_t^C		1.492	5.407		1.377	4.169
		Coherence	C_t^C	0.569		2.441	0.585		1.116
			P_t^C	0.727	0.426		0.628	0.405	
4. Diagnostics									
	Y_t	C_t	P_t	Y_t	C_t	P_t	Y_t	C_t	P_t
LL			2035.197			2055.486			2057.606
R_D^2	0.297	0.405	0.602	0.324	0.412	0.641	0.338	0.414	0.648
$Q(20)$	19.042	17.914	*31.578	19.075	17.910	*37.267	19.401	17.952	*35.195
5. Likelihood ratio tests									
a) $\phi_1 = \phi_2 = \phi_3 = 0$			**91.989						
b) Similar Cycles (Y, C, P)			*15.350						
c) Similar Cycles (C, P)			1.163						

For notation see section A1. For credit we used one dummy to account for an additive outlier in 1976Q2, and two dummies to account for level shifts in 1977Q4 and 1980Q1. For house prices we used three dummies to account for additive outliers in 1976Q2, 1980Q1 and 1991Q4.

Table A.6: Main Parameter Estimates Spain

	Univariate			Multivariate Restricted slopes			Multivariate Estimated slopes		
1. Trend parameters									
	Y_t	C_t	P_t	Y_t	C_t	P_t	Y_t	C_t	P_t
$\sigma_\eta \times 100$	0.000	0.000	0.861	0.427	0.109	0.450	0.426	0.108	0.459
$\sigma_\zeta \times 100$	0.050	0.250	0.100	0.052	0.250	0.100	0.043	0.250	0.025
2. Parameters stochastic cycles									
	$\psi_{1,t}$	$\psi_{2,t}$		$\psi_{1,t}$	$\psi_{2,t}$		$\psi_{1,t}$	$\psi_{2,t}$	
ϕ	0.150	0.697		0.000	0.842		0.000	0.857	
ρ	0.980	0.980		0.936	0.980		0.937	0.980	
$2\pi/4\lambda$	14.767	16.998		3.331	18.917		3.343	20.328	
3. Cyclical components									
	Y_t	C_t	P_t	Y_t	C_t	P_t	Y_t	C_t	P_t
$2\pi/4\lambda^G$	12.266	15.627	15.627	17.582	18.690	17.075	19.043	20.148	18.579
$\sigma^C \times 100$	3.021	8.050	23.173	4.118	14.038	21.191	4.580	15.428	23.581
					Phase			Phase	
				Y_t^C	C_t^C	P_t^C	Y_t^C	C_t^C	P_t^C
			Y_t^C		2.959	-0.387		3.097	-0.228
		Coherence	C_t^C	0.808		-7.116	0.807		-6.026
			P_t^C	0.740	0.437		0.775	0.459	
4. Diagnostics									
	Y_t	C_t	P_t	Y_t	C_t	P_t	Y_t	C_t	P_t
LL			2091.669			2119.325			2119.417
R_D^2	0.283	0.850	0.561	0.369	0.862	0.571	0.372	0.862	0.569
$Q(20)$	28.100	*34.147	25.159	24.692	**42.344	*35.387	24.614	**43.231	**34.438
5. Likelihood ratio tests									
a) $\phi_1 = \phi_2 = \phi_3 = 0$				**68.912					
b) Similar Cycles (Y, C, P)				**24.586					
c) Similar Cycles (C, P)				2.932					

For notation see section A1. We used use two dummies to account for additive outliers in credit in 1986Q1 and 1999Q2, and one dummy to account for a level shift in house prices in 1991Q4.

Figure A.1: Trend-Cycle Decomposition United States

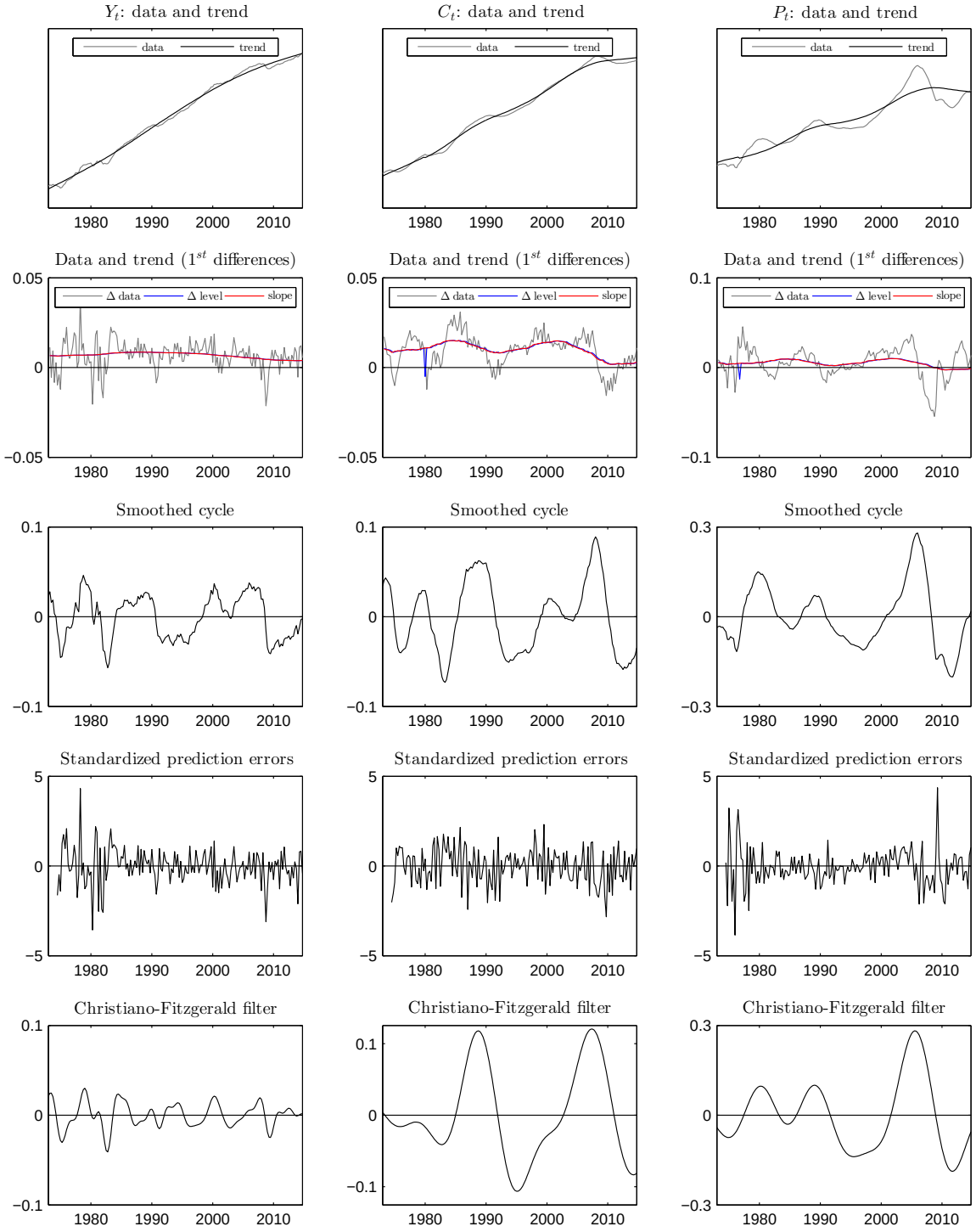

Figure A.2: Trend-Cycle Decomposition United Kingdom

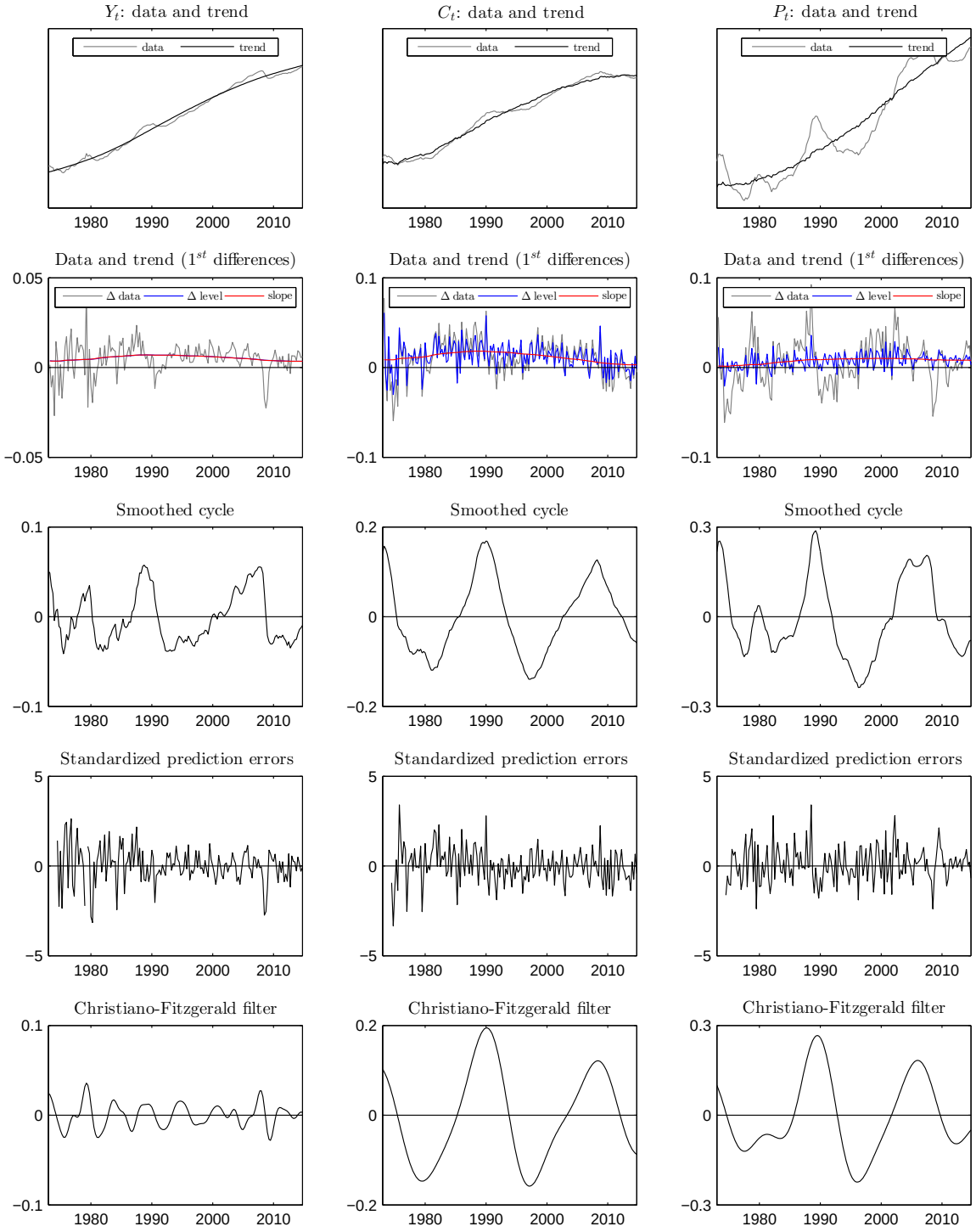

Figure A.3: Trend-Cycle Decomposition Germany

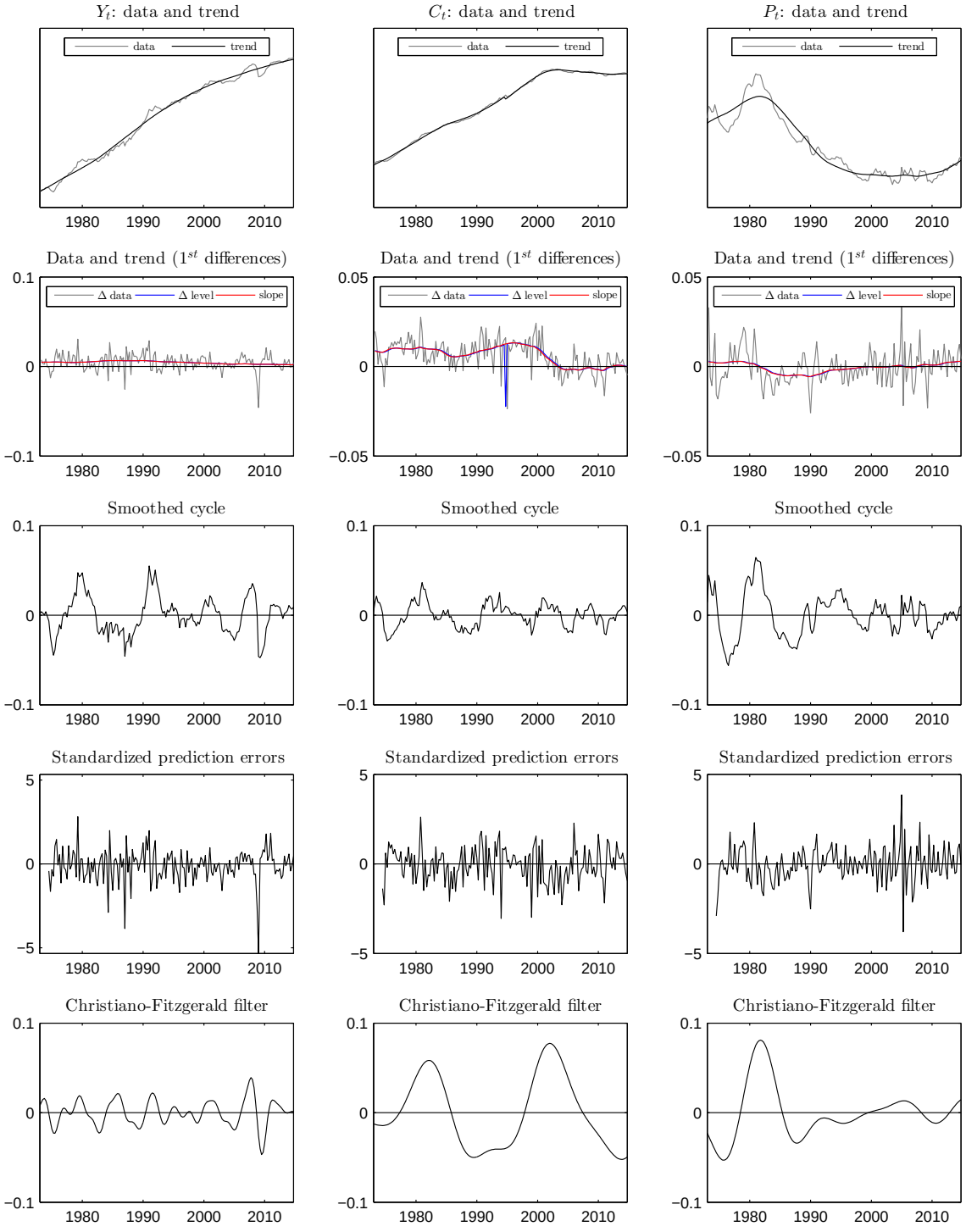

Figure A.4: Trend-Cycle Decomposition France

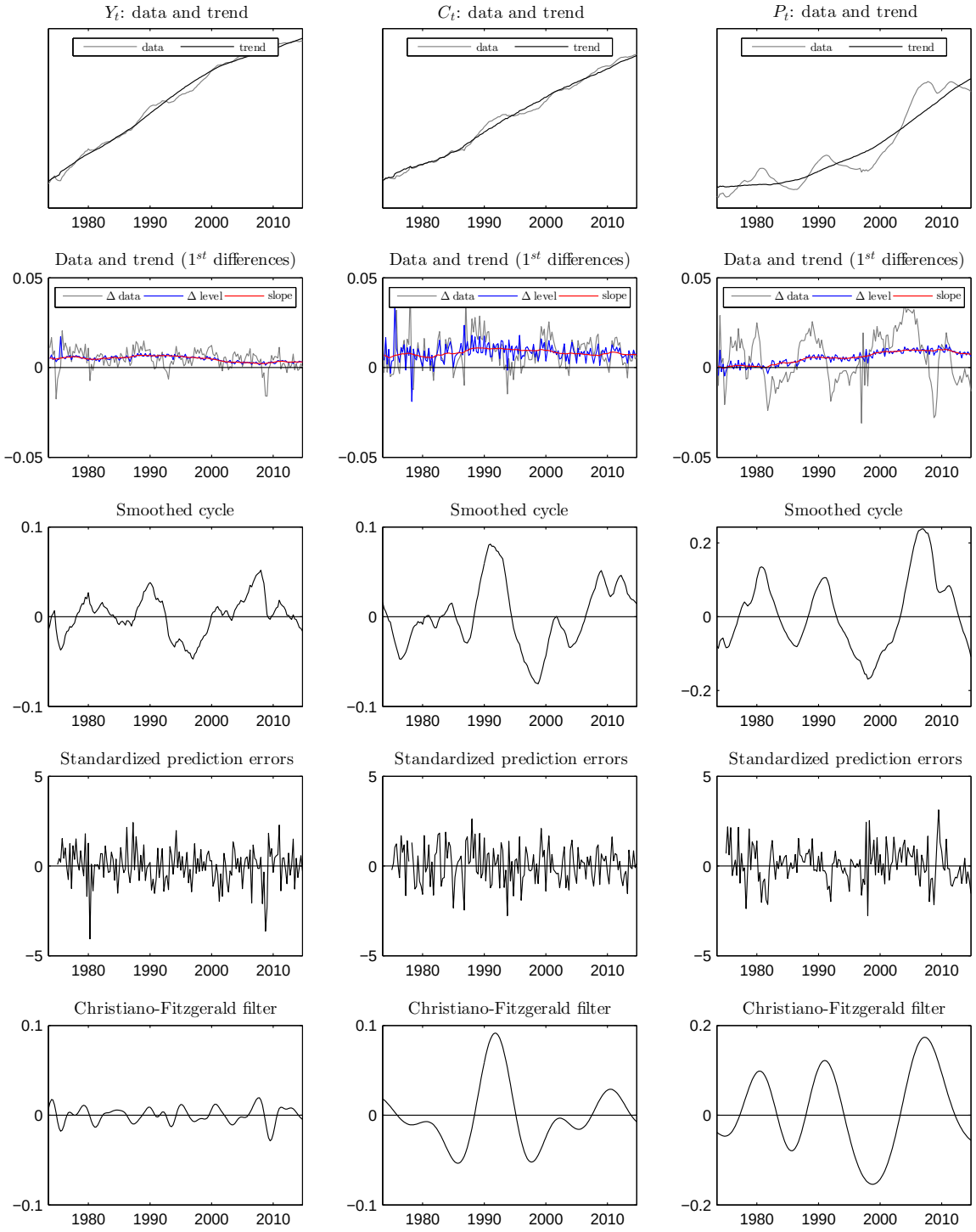

Figure A.5: Trend-Cycle Decomposition Italy

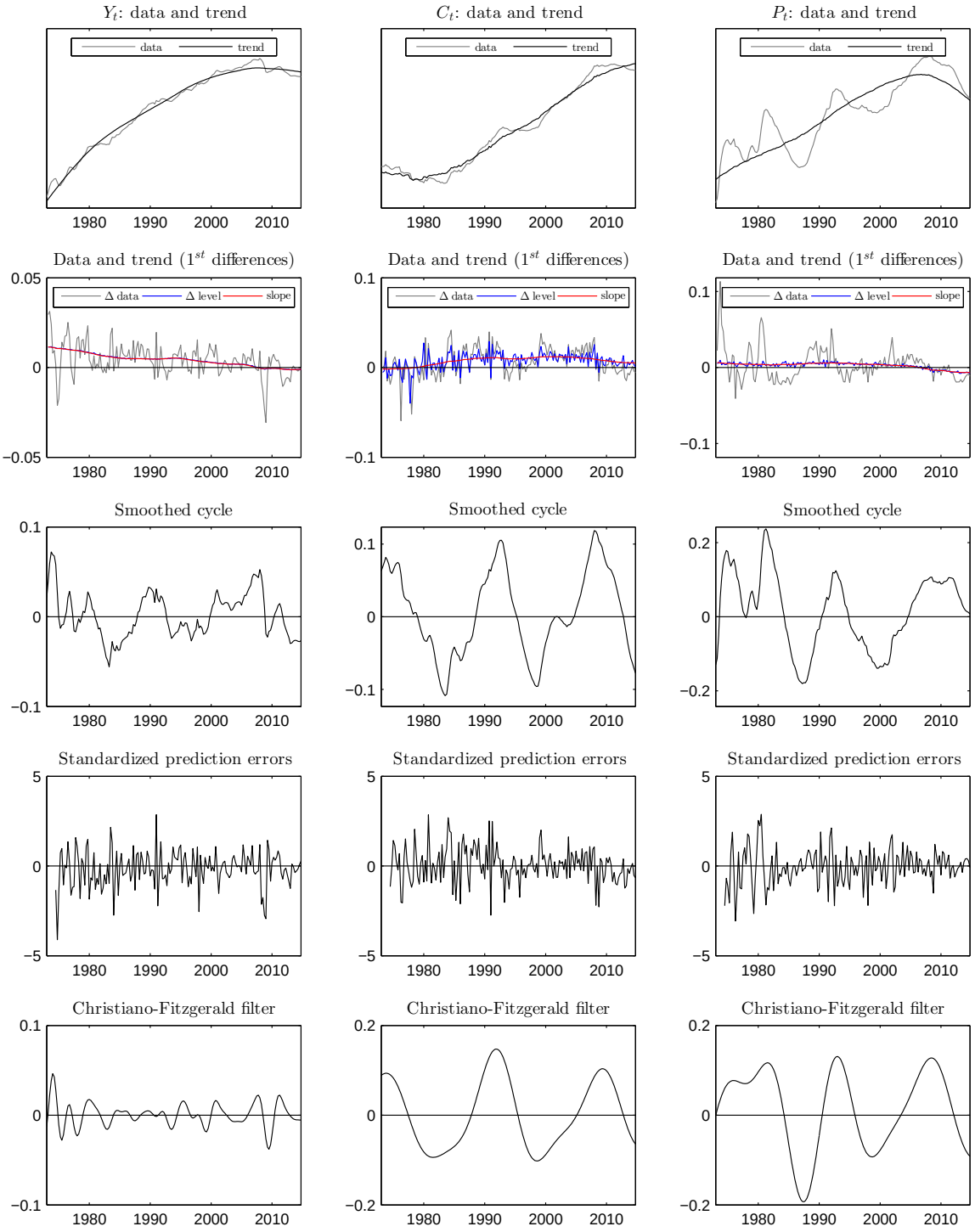

Figure A.6: Trend-Cycle Decomposition Spain

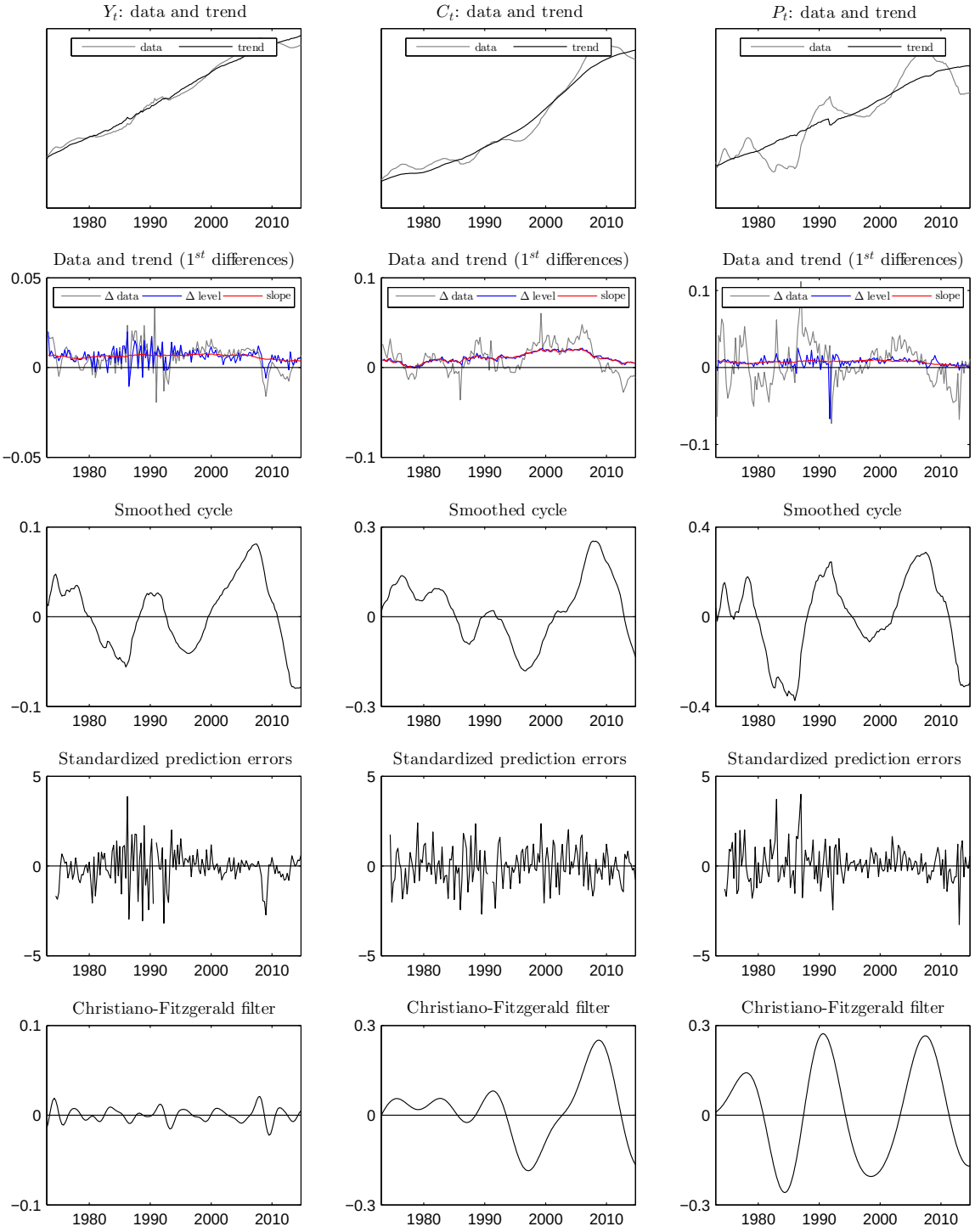

Figure A.7: Spectral Characteristics of Cycles United States

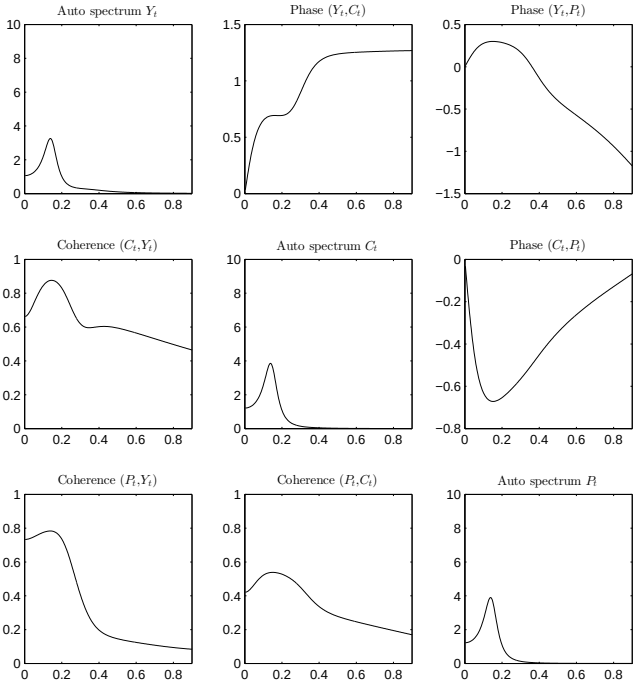

Figure A.8: Spectral Characteristics of Cycles United Kingdom

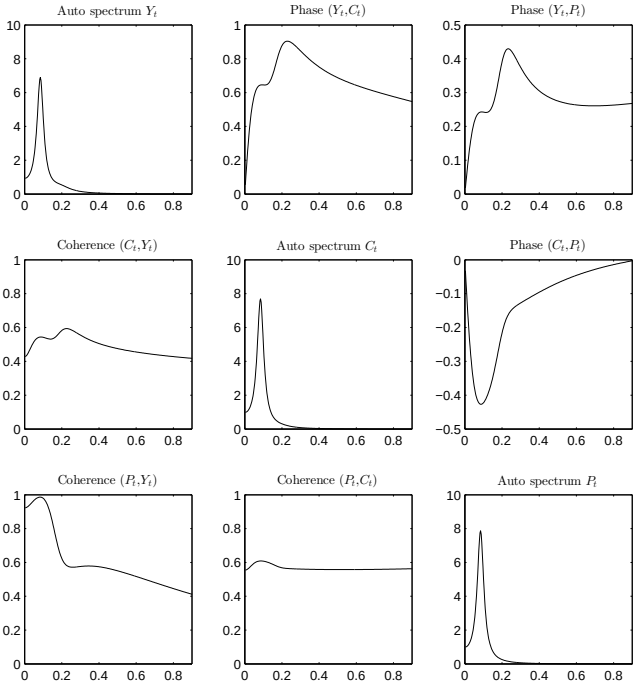

Figure A.9: Spectral Characteristics of Cycles Germany

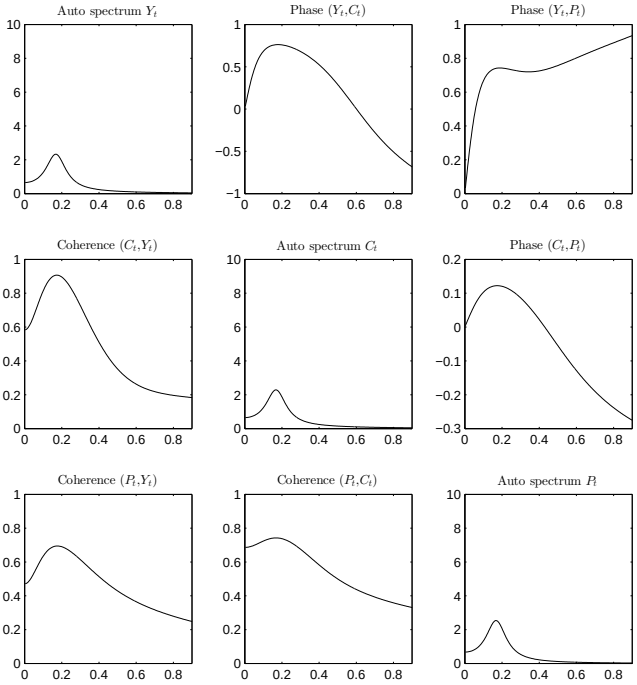

Figure A.10: Spectral Characteristics of Cycles France

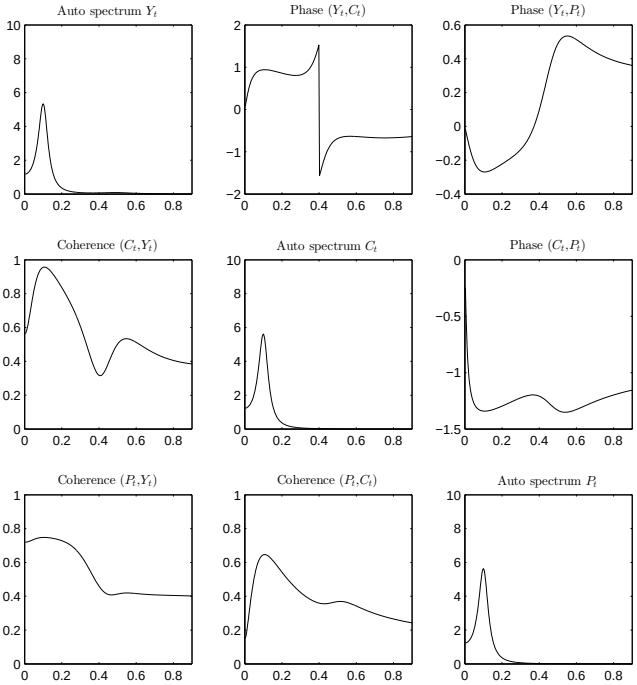

Figure A.11: Spectral Characteristics of Cycles Italy

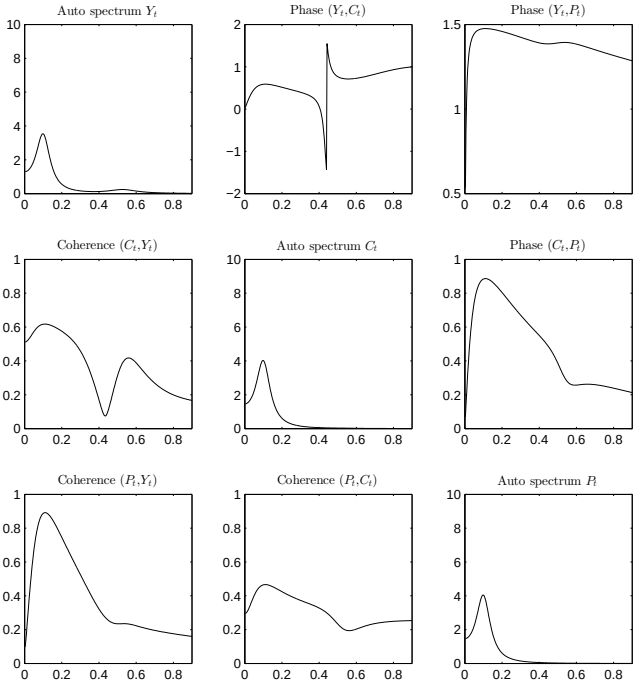

Figure A.12: Spectral Characteristics of Cycles Spain

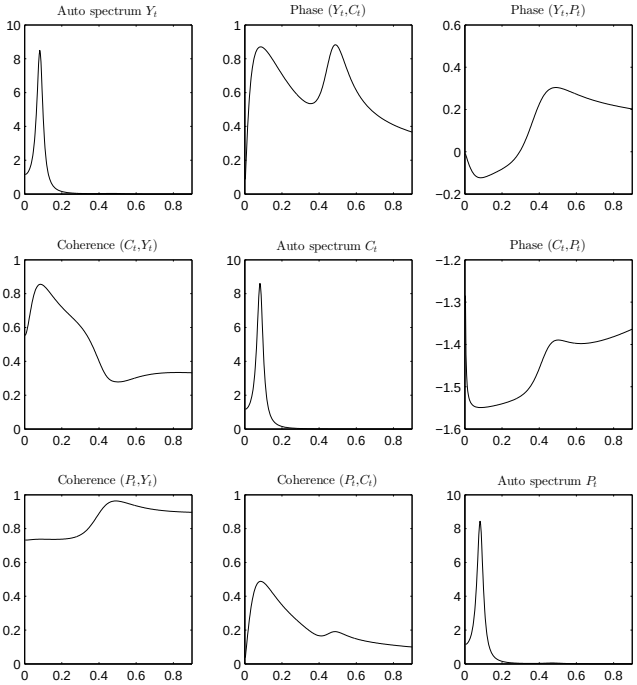

Supplement B: Comparison with other Estimates

Figure B.1: Smoothed Cycles, Christiano-Fitzgerald Filter

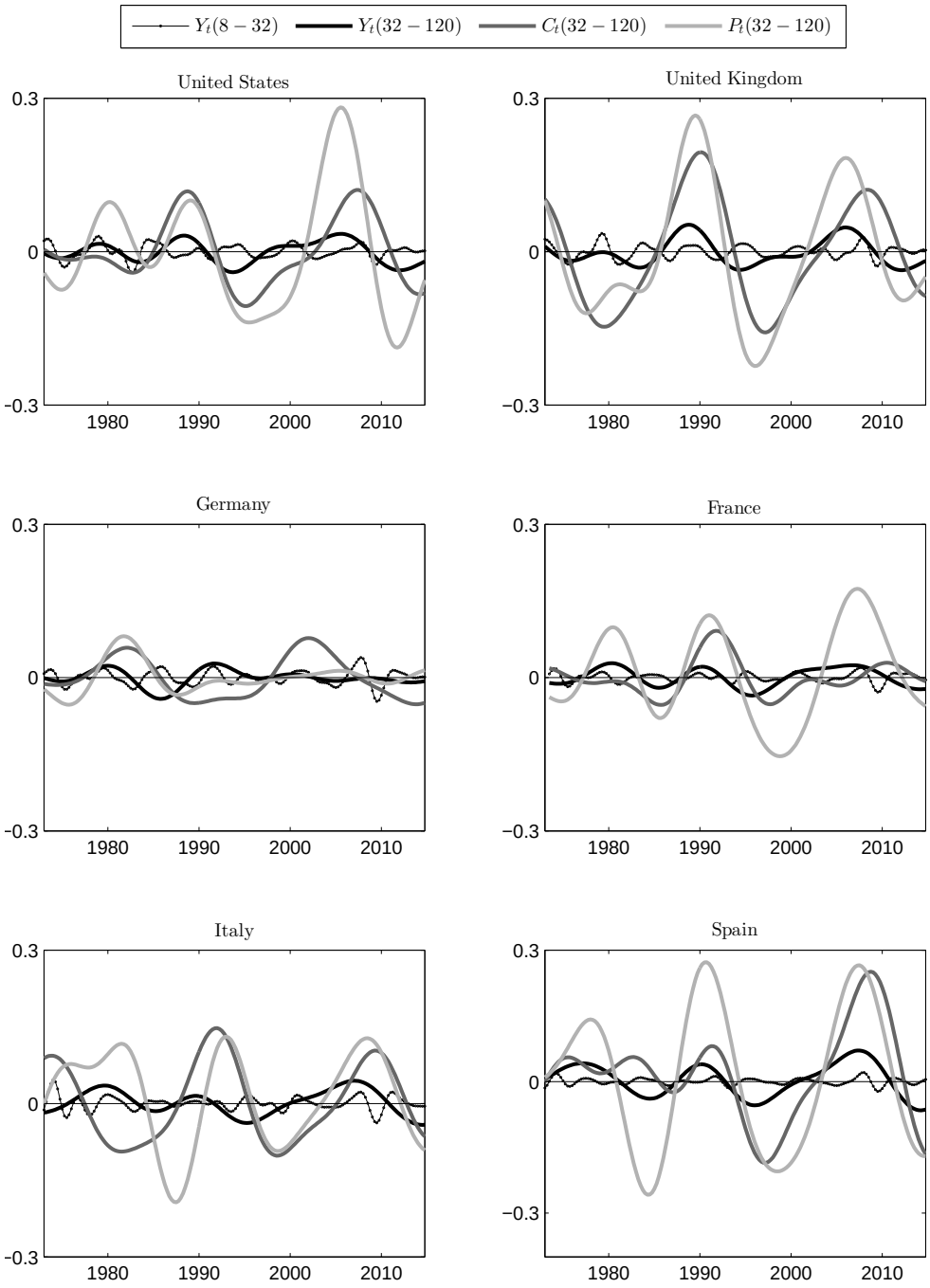

Figure B.2: Estimates of GDP Cycles from Various Sources

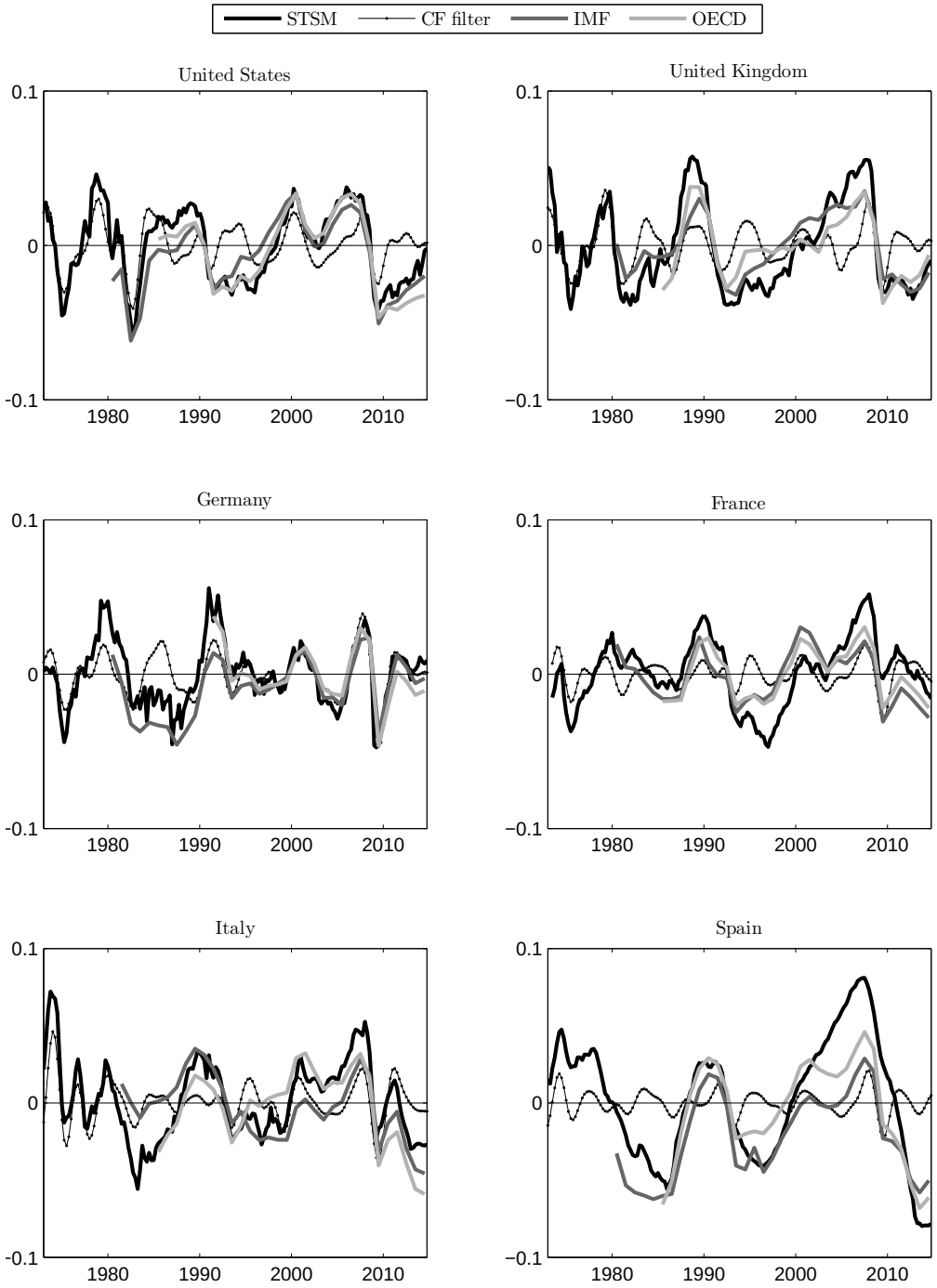

Table B.1: CF Filter Sample Correlations for Short- and Medium-Term Cycles

		$\widehat{\sigma}^C$ (8-32)	$\widehat{\sigma}^C$ (32-120)			8-32		
U. S.						Y_t^C	C_t^C	P_t^C
	Y_t	1.379	2.133		Y_t^C		0.829	0.536
	C_t	1.747	6.359	32-120	C_t^C	0.800		0.441
	P_t	2.550	11.684		P_t^C	0.830	0.763	
U. K.						Y_t^C	C_t^C	P_t^C
	Y_t	1.297	2.570		Y_t^C		0.660	0.710
	C_t	2.452	10.198	32-120	C_t^C	0.777		0.410
	P_t	4.139	12.734		P_t^C	0.904	0.922	
Germany						Y_t^C	C_t^C	P_t^C
	Y_t	1.440	1.540		Y_t^C		0.573	0.416
	C_t	0.936	4.006	32-120	C_t^C	0.562		0.444
	P_t	1.234	2.925		P_t^C	0.932	0.581	
France						Y_t^C	C_t^C	P_t^C
	Y_t	0.875	1.806		Y_t^C		0.644	0.605
	C_t	1.263	3.435	32-120	C_t^C	0.687		0.535
	P_t	2.219	8.985		P_t^C	0.788	0.586	
Italy						Y_t^C	C_t^C	P_t^C
	Y_t	1.311	2.382		Y_t^C		0.409	0.409
	C_t	1.741	7.561	32-120	C_t^C	0.462		0.329
	P_t	3.797	8.852		P_t^C	0.615	0.590	
Spain						Y_t^C	C_t^C	P_t^C
	Y_t	0.759	3.688		Y_t^C		0.387	0.486
	C_t	1.989	10.199	32-120	C_t^C	0.835		0.163
	P_t	3.674	15.976		P_t^C	0.865	0.700	

The first two columns show the sample standard deviations of the cycles extracted with a CF filter with frequency bands of 8-32 and 32-120 quarters, respectively. The right-hand panel shows the maximum value of sample cross-correlations between cycles (of all leads and lags). The lower left of the matrix shows the statistics for the 32-120 quarter frequency band, while the upper right shows those for the 8-32 quarter frequency band.